DEMOCRATIC PEOPLE's REPUBLIC OF ALGERIA
MINISTRY OF HIGHER EDUCATION AND SCIENTIFIC RESEARCH

UNIVERSITY OF MEDEA
FACULTY OF SCIENCE



Thesis

Presented to obtain the **Master's** degree
In physics

Speciality : **Physics of materials**

By :
DEBOUB Nabila

Thesis title :

Theoretical Investigation and Characterization of a Magnetic Heusler Alloy of Composition X_2MnM with Co_2MnGe as Prototype.

presented and supported at Medea , June 20, 2018.

Board of examiner

MEDIA El Mahdi	MAA	University of Medea	President
GUECHI Nacir	MCA	University of Medea	Examiner
LACHENANI Hanane	MAA	University of Medea	Examiner
DEHBAOUI Mourad	MCA	University of Medea	Supervisor

YEAR : 2017/2018

Dedication

I dedicate this work,

To the man who raised me in the hardest times -my beloved father-,
To the loving memory of my mother,
you have successfully made me the person I am becoming, you will always be remembered.
To my brothers and sisters,
To all of my friend,

To those who support me.



Acknowledgement

This work in physics of materials was carried out in the computer lab of Sciences Department at the University of Medea under the direction of Mr.Dr.M.DEHBAOUI.

First of all, I would like to express my deepest gratitude to Dr.M.DEHBAOUI for the trust he gave me to carry out this work under his direction. Also, i want to thank him for his guidance, patience and his wisdom advice that has been invaluable on both academic and personal level. I thank him for all the efforts he has made in order to get this work to the light.

I have a great deal of appreciation for Mr.Dr.N. GUECHI for his guidance throughout my research. His great scientific background in the calculation method was a decisive factor in the development of this work. I'd like to thank him for his idea and the discussion we had.

And not to forget Mrs.H.Lachenani for her support in the DFT part with her reference and explanation. Also i'd like to thank Dr.A.BOUKAOUD for his help and support.

Finally, thank to all those who have collaborated closely or from afar with the result of this work, may they accept my thankful word. And last but not the least my grateful thanks go to all the teachers of the sciences department specially the physics of material branch.

Contents

i. General introduction 1

I Generalities on magnetism 4

1 Class of magnetism . . . 5

1.1 Diamagnetism . . . 5

1.2 Paramagnetism . . . 6

1.3 Ferromagnetism . . . 6

1.4 Antiferromagnetism . . . 6

1.5 Ferrimagnetism . . . 7

2 Localized and itinerant magnetism . . . 7

3 Hysteresis loop . . . 8

4 Magnetic anisotropy . . . 9

4.1 Magneto-crystalline anisotropy (MCA) . . . 10

4.2 Shape anisotropy . . . 10

4.3 Stress anisotropy . . . 10

5 Exchange interaction . . . 10

II Heusler alloys 12

1 Crystal structure of Heusler alloys . . . 14

2 Half-metallicity of the Heusler alloys . . . 16

3 Origin of half-metallic gap . . . 17

4 Magnetic properties . . . 20

4.1 Slater-Pauling behaviour . . . 20

4.2 Exchange interactions . . . 23

III Overview of theoretical framework 24

1 Density Functional Theory . . . 24

1.1 Elementary quantum mechanics . . . 24

1.1.1 Schrödinger equation 24
1.1.2 Born-Oppenheimer approximation 25
1.1.3 The variational principle for the ground state 26
1.1.4 The Hartree-Fock approximation 26
1.2 Density functional theory 27
1.2.1 Hohenberg-Kohn theorems 28
1.2.2 Kohn-Sham equation 28
1.3 The exchange-correlation functional 29
1.3.1 Local density approximation(LDA) 29
1.3.2 Local spin density approximation(LSDA) 30
1.3.3 The generalized gradient approximation(GGA) 30
1.3.4 Perdew-Burke-Ernzerh approximation(GGA-PBE) . . 31
1.4 Resolution of Kohn-Sham equation 31
2 The Pseudo-potential method (PP) 33
2.1 Bloch's theorem and plane waves 33
2.2 Integration of the Brillouin zone and k points 34
2.3 General approximation 34
2.3.1 Norm-conserving Pseudo-potential 35
2.3.2 Pseudo-potential ultra-soft (US-PP) 35

IV Results and discussions **36**
1 Computational details 36
2 Structural properties 37
2.1 Crystal structure of Co_2MnGe 37
2.2 Effect of pressure on the volume and lattice parameter 40
3 Electronic properties 41
3.1 Brillouin zone 41
3.2 Band structure 42
3.3 Effect of pressure on the energy gap 43
3.4 Total and partial densities of states 45
4 Magnetic properties 47
4.1 Effect of pressure on the magnetic moment 47
4.2 Spin polarization 48
4.3 Effect of pressure on spin polarization 49
5 Conclusion 50

***c.* General Conclusion** **51**

Bibliography **53**

List of Figures

I.1 Magnetic periodic table. 5
I.2 Representation of magnetic moment in diamagnetic and paramagnetic materials. 6
I.3 Representation of magnetic moment in ferromagnetic, antiferromagnetic and ferrimagnetic materials. 7
I.4 Magnetic hysteresis loop and initial magnetization curve showing saturation magnetization, saturation remanence, coercivity, remanence coercivity and low field magnetization changes. 9

II.1 Periodic table of the elements. The huge number of Heusler materials can be formed by combination of the different elements according to the colour scheme. 13
II.2 Schematic representations of the various structures of the Heusler compounds. In all cases the lattice is consisted of four interpenetrating fcc lattices. Note also that if all atoms were identical, the lattice would be simply the bcc. 14
II.3 Schematic representation of the density of states for a half-metal with respect to normal metals and semiconductors. 16
II.4 Calculated spin-projected density of states (DOS) for Co_2MnSi and Co_2MnGe. The band gap at the Fermi level for the minority spin band is clearly evidenced 16
II.5 Shapes of d-orbitals. 17
II.6 Splitting of d-orbitals. Where 10 Dq or Δ_0 is the energy separation between the two levels, 6 Dq is the amount of repulsion energy needed by e_g orbitals, -4Dq is the stabilization extent needed by t_{2g} orbitals with respect to the barycenter.(Octahedral symmetry) . . . 18

II.7 Schematic illustration of the origin of gap in the minority spin band in full-Heusler alloys. For legibility reasons, we use $d1$,$d2$ and $d3$ to denote the d_{xy},d_{yz} and d_{zx} orbitals, respectively, and $d4$,$d5$ for the d_z^2,$d_{x^2-y^2}$ orbitals.(adopted from [24]) 19
II.8 Slater-Pauling curve for 3d transition metals and their alloys. Experimental values for selected Co based Heusler alloys and for binary alloys are also given. 21
II.9 Left panel : Calculated total magnetic moment as a function of the total number Z_t of valence electrons per unit cell for all the studied half Heusler alloys. The dashed line represents the Slater-Pauling behaviour. The open circles present the compounds deviating from the SP curve. Right panel : The same for the full Heusler alloys. . . 22

III.1 Schematic representation of the self-consistent cycle in the framework of DFT. 32
III.2 Forms of valence wave functions, pseudo-function, potential of all valence electrons and Pseudo-potential as a function of the atomic radius r. 35

IV.1 Structure of Co_2MnGe compound, conventional (left) and primitive cell (right). 37
IV.2 Crystal structure of Co_2MnGe ternary Heusler compound for (a)-Type I, (b)-Type II, (c)-Type III. 38
IV.3 Total energy as a function of unit volume cell for Co_2MnGe in it's most stable phase I. 39
IV.4 Lattice parameter (a) and volume (b) of the primitive cell versus pressure. 40
IV.5 Brillouin zone of the Co_2MnGe compound; g_1,g_2 and g_3 are the reciprocal space vectors. 42
IV.6 Band structures curves for Co_2MnGe calculated at zero pressure. . 42
IV.7 Band structure of minority spin under different pressure. 44
IV.8 Variation of the energy gap as a function of pressure. 45
IV.9 The total and partial density of states (DOS's) for Co_2MnGe at 0 GPa. 46
IV.10 Total (a) and Partial (b) magnetic moment as function of pressure. 48
IV.11 The amplified curves of the DOS for Co_2MnGe near the Fermi level. 49
IV.12 The curves of spin polarization for Co_2MnGe as function of pressure. 50

List of Tables

II.1 Inequivalent site occupancies within the C1b-type structure. Atoms on Wyckoff positions 4a and 4c form ZnS-type sublattices; the atoms on 4b occupy the octahedral holes. 15

IV.1 Atoms positions in three possible configurations for Co_2MnGe compound. 37

IV.2 Lattice constants and the equilibrium energy values for the three different configurations. 38

IV.3 The calculated bulk parameters of Co_2MnGe in it's most stable phase I. 40

IV.4 Calculated values of the total and partial magnetic moment in Co_2MnGe. 47

IV.5 Calculated total magnetic moment (in μ_B) and spin polarization (P) for Co_2MnGe (5^c represent the present calculation). 48

IV.6 Prominent value of spin polarization as function of pressure. 49

List of Abbreviations

CASTEP ..... Cambridge Serial Total Energy Package

MCA ..... Magneto-Crystalline Anisotropy

RKKY ..... Ruderman Kittel Kasuya Yosida

MRAM ..... Magnetic Random Access Memories

fcc ..... face centred cubic

bcc ..... basis centred cubic

DOS ..... Density Of States

VBT ..... Valence Bond Theory

CFT ..... Crystal Field Theory

TM ..... Transition Metal

SP ..... Slater Pauling

DFT ..... Density Functional Theory

LDA ..... Local density approximation

LSDA ..... Local spin density approximation

GGA ..... The generalized gradient approximation

PBE ..... Perdew-Burke-Ernzerh

SC ..... self-Consistent

PP ..... Pseudo-potential

BZ ..... Brillouin Zone

US-PP ..... Pseudo-potential ultra-soft

MEOS ..... Murnaghan Equation Of States

HMF ..... Half-Metallic Ferromagnets

EF ..... Energy Fermi

Introduction *i.*

General introduction

The invention of the bipolar transistor in 1947, by John Bardeen, Walter Brattain and William Shockley, opened the era of microelectronics, a discipline interested in the study and manufacture of electronic components at the micrometric scale [5]. The displacement of electrons are no longer performed in a vacuum, but in a solid material with the ability to control electron currents. Components are made from semiconductors materials using various technologies, including photolithography. The transistors are made directly on the surface of the semiconductor ; their connections are made by deposition of metal layers. Electronics technology continued to develop and saw itself split into two broad areas of application : a first domain connected to the charge, which is responsible for the process of transporting information and communication, a second domain related to the spin, which is responsible for the storage of information.

Intensified studies in Nano metric magnetism have led to a remarkable progress in the applications of magnetism in different fields. The technical progress recently made in the preparation of multilayers of thin films and nanotubes has led to the discovery of giant magnetoresistance in 1988 [6]. The discovery led to the development of magnetic sensors and the emergence of a new generation of electronics : the spintronics. Spintronics is a branch of fast developing electronics that combines the knowledge of spin physics and magnetism with electronics and optics in new multifunctional devices. Adding the spin degree of freedom to the conventional electronic devices has several advantages like non-volatility, increasing data processing speed, decreasing electric power consumption and increasing integration densities [7]. The evolution of research and studies have been expanded to discover new type of material which have the potential for advanced sensor and memory application and exhibit half-metallicity nature, a phenomenon with a great intensity in the development of materials, a new class of materials has been predicted, the so-called half-ferromagnetic metals.

One of the candidate for this discipline are the Heusler alloys, trying to combine in their functionalities the two degrees of freedom (spin and charge) of the electron. For the time being Spintronic involves the study of an active control and manipulation of the spin via the control of the spin flow in the Heusler materials for the sake of an advanced magnetic memory and sensors based on spin transport electronics.

The history of Heusler alloys begin back in 1903 when Fritz Heusler discovered that an alloy with the composition Cu_2MnAl behaves like a ferromagnet, although non of its constituent elements is ferromagnetic by itself [8]. With the discovery of half-metallic ferromagnetism in $NiMnSb$ [9] with a particular crystalline structure (Semi-Heusler structure), The Heusler alloys received tremendous experimental and theoretical interest in order to design new compounds. Numerous studies predict the half metallicity character and the high Curie temperature for the Heusler containing the cobalt and manganese [4]. In the half-metallic materials, the two spin bands show a completely different behaviour. The majority spin band shows the typical metallic behaviour, and the minority spin band exhibits a semiconducting behaviour.

More detailed study and investigation are necessary to develop this kind of material. In this work, we have interested in the Co_2MnGe prototype of full Heusler alloys. Because of their relatively high Curie temperature (Tc= 883 K [10]) and high spin polarization (P=100% [10]), the material gained great attention from the experimental and theoretical investigations.

In this work we have used ab-initio methods to study the effects of pressure on the structural, electronic and magnetic properties of the of Co_2MnGe compound. The investigation is held using the Density Functional Theory calculation with Pseudo-potential approximation implemented in the Material studio CASTEP code.

The dissertation is organized into four chapters : After an introductory section, we discuss in the first chapter a general overview on the origin of magnetism and the classification of materials based on their magnetic behaviour. In the second chapter, we introduce generality on the Heusler alloys and their properties, where we present the development of this class of material and present their different types and applications. In chapter three, a theoretical background is presented ; Density functional theory is a promising method for characterising materials is put under light, their main theorems and approximations are discussed, a Pseudo-potential approximation implemented with CASTEP code is also introduced.In chapter four, the mains results of theoretical calculation based on the structu-

ral, electronics and magnetic properties are presented and discussed in detail. A conclusion and future prospects are summarized at the end of the dissertation.

Chapter I

Generalities on magnetism

Introduction

The magnetism in solids takes it's origin from two type of motions of electron in atoms, one is the orbital motion of the electron around the nuclei, the other is the spin of the electron around its axis. The orbital and the spin motion independently impart a magnetic moment on each electron causing each of them to behave as a tiny magnet [11]. In a large fraction of the elements, the magnetic moment of the electrons cancel out because of the Pauli exclusion principle (two or more identical fermions can not occupy the same quantum states within quantum system simultaneously). Therefore, most of the magnetic moments originated from spins cancel each other and does not contribute to the magnetic moment of a solid [12]. However, several materials (transition metal), have a net magnetic moment due to the spin of electron. The magnetism in solids depends on how these atomic magnetic moments are aligned in crystals, which lead to five main classification of magnetic that have a prominent role in applications of magnetic materials : diamagnetism, paramagnetism, ferromagnetism, ferrimagnetism and antiferromagnetism.

1 Class of magnetism

The magnetism of solids depends on how the magnetic moments are aligned, there are five basic types of magnetism have been observed and classified. The two most common type of magnetism are diamagnetism and paramagnetism, which represent the large number of periodic table elements at room temperature (See figure I.1). These elements are usually referred as a non-magnetic, while the magnetic elements are classified in the ferromagnetism, Anti-ferromagnetism and ferrimagnetism classes. Ferrimagnetic properties are not observed in any pure element but can only be found in compounds, such as the mixed oxides, known as ferrites.

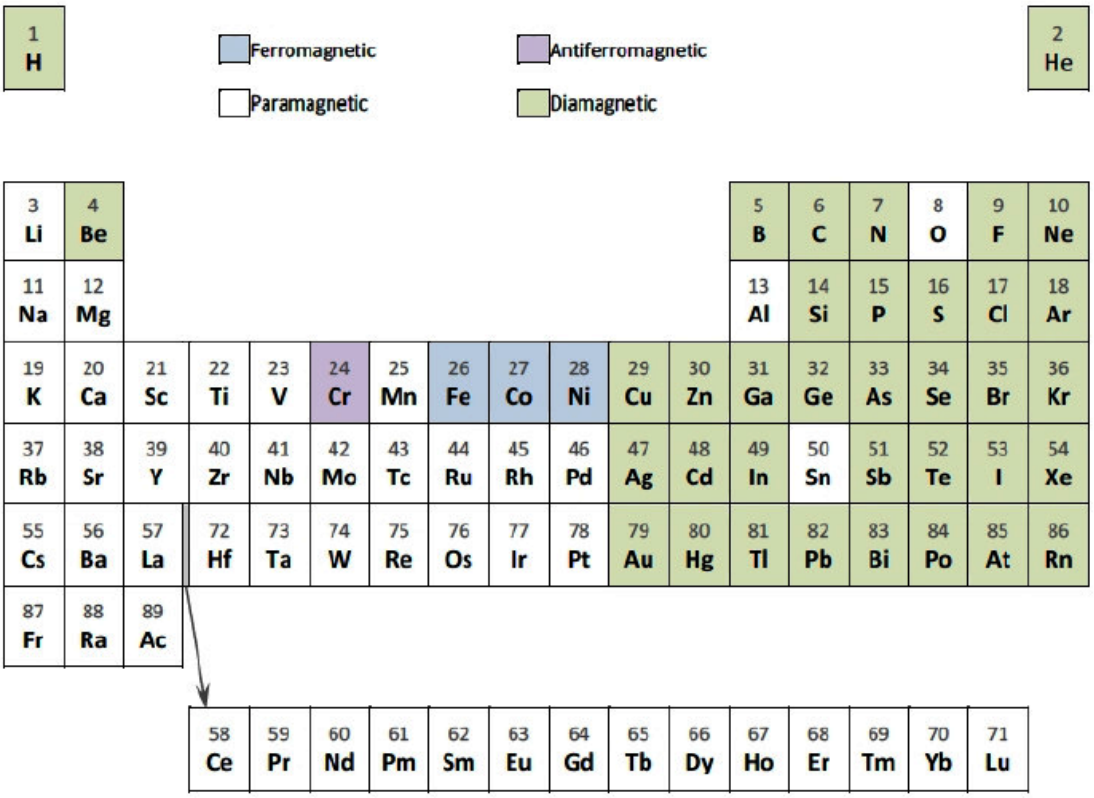


Fig. I.1 – Magnetic periodic table. (adopted from [1])

.

1.1 Diamagnetism

In some materials the application of magnetic field induces a very small magnetic moment in the direction which is opposite to the applied magnetic field (see figure I.2-left panel). The induced magnetic moment will disappear as soon as the applied magnetic field is removed. This phenomenon is known as diamagnetism. The spin magnetic moment doesn't contribute to the magnetization of diamagnetic materials, all the spin motions are paired and the spin moments cancel each

other.

1.2 Paramagnetism

In paramagnetic materials there is a magnetic moment with no ordering at finite temperature leading to zero net magnetization in the absence of magnetic field. These magnetic moments have a tendency to align along the direction of the applied magnetic field leading to a finite magnetization in applied magnetic field (see figure I.2-right panel). A paramagnetic system with localized magnetic moments obeys Curie's law which states that the magnetic susceptibility (χ) is inversely proportional to the temperature.

$$\chi = \frac{C_{curie}}{T} \tag{I.1}$$

where C_{curie} is a material-specific Curie constant.

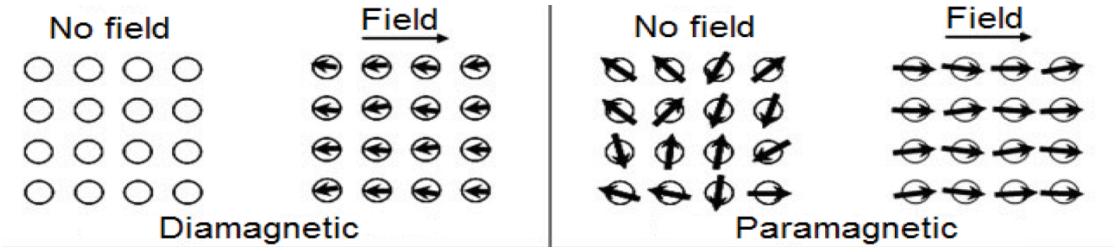


Fig. I.2 – Representation of magnetic moment in diamagnetic and paramagnetic materials.

1.3 Ferromagnetism

A ferromagnetic material has a spontaneous magnetization even in the absence of an applied magnetic field (see figure I.3-left panel) due to magnetic phenomenon of positive exchange interaction between neighbouring moments causing the alignment of magnetic moments in parallel arrangement to each other. This effect is explained in classical theory by the presence of a molecular field within the ferromagnetic material, which was first postulated by Weiss in 1907. While in quantum mechanics, the Heisenberg model of ferromagnetism describes the parallel alignment of magnetic moments by the exchange interaction phenomenon.

1.4 Antiferromagnetism

When the exchange parameter is negative, neighbouring magnetic moments are aligned anti-parallel and the resultant order is known as the antiferromagnetic order (see figure I.3-right panel). Very often in an antiferromagnetic material there

are two sub-lattices with equal magnetic moments pointing in opposite directions. Each of the sub-lattices has a spontaneous magnetization even in the absence of an applied magnetic field just like a ferromagnet.

1.5 Ferrimagnetism

Ferrimagnetism is observed in compounds with more complex crystal structures than the single elements. Where two sub-lattices, with opposite magnetic order, do not have an equal magnetic moments and ordering a parallel alignment of atoms in some of the crystal sites and anti-parallel alignment in the others (see figure I.3-central panel). Then, contrary to the case of an antiferromagnet, the net magnetization is not zero. The material breaks down into magnetic domains, just like a ferromagnetic material and the magnetic behaviour is also very similar.

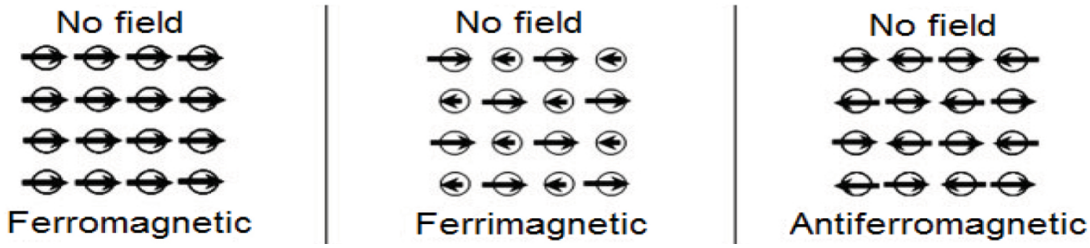


Fig. I.3 – Representation of magnetic moment in ferromagnetic, antiferromagnetic and ferrimagnetic materials.

2 Localized and itinerant magnetism

The description of the magnetism of atoms constituting of different substance is much more complex than that of the magnetism of the free atoms, because it's a problem with N body that it is impossible to be exactly solved. Two different models have been developed : localized and itinerant magnetism where both of them rate as approximations [13].

The first model considers the material as a collection of magnetic moments, the electron who is responsible for these moments remain perfectly localized around their original kernel and are in an electronic states quite close to that of the atom or free ion. Such atoms/ions in the system are called magnetic ions. 3d transition metal oxide insulators and rare earth metals and their intermetallic compounds are examples of such systems. At the opposite side, in the itinerant magnetism, the electrons carrying the magnetic moments are not localized to atoms in solid and can move from one location to another inside the solid (electrons relocated and free to travel in all direction). Fe, Ni and Co are examples of such systems.

3 Hysteresis loop

The magnetic hysteresis loop or as it is known B-H curve is obtained by plotting the induced magnetic flux density (B) and the magnetizing force (H) as it is shown in figure I.4. The loop is generated by measuring the magnetic flux of a ferromagnetic or ferrimagnetic materials while the magnetizing force is changed. The flux density increases in proportion to the field strength until it reaches a certain value were it can not increase any more becoming almost level and constant as the field strength continues to increase. The material has reached the point of magnetic saturation also known as Saturation of the core (point "a" in figure I.4). As the magnetic flux is reduced to zero, the curve move from point "a" to point "b". However, the magnetic flux does not completely disappear even if the magnetizing force is zero, corresponding to the retentivity or the remanence. By reversing the magnetizing force, the curve move toward point "c", where the flux is reduced to zero and the magnetic field change direction. The point "c" correspond to the coercive force or coercivity of the material.If this reverse magnetizing force is increased further the flux density will also increase in the reverse direction until it reaches the saturation point "d" in the opposite direction. Reducing H once again to zero will produce an amount of residual magnetism equal to that achieved in the other direction. Again increasing H back in the positive direction will cause the magnetic flux to reach zero point "f", and as before increasing the magnetizing force further in a positive direction will cause the core to reach saturation at point "a".

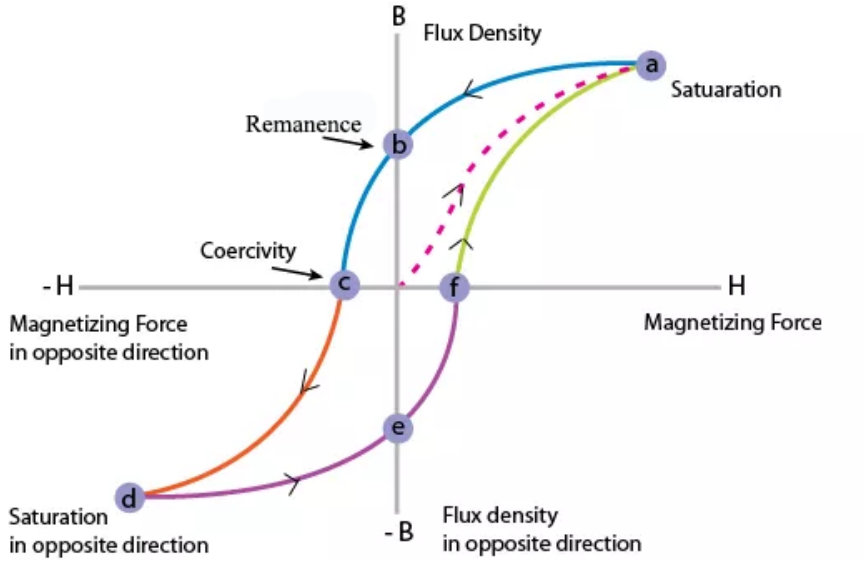


Fig. I.4 – Magnetic hysteresis loop and initial magnetization curve showing saturation magnetization, saturation remanence, coercivity, remanence coercivity and low field magnetization changes.

Some ferromagnetic materials have a high coercivity (magnetically hard) making them excellent for producing permanent magnets. While other ferromagnetic materials have low coercivity (magnetically soft) making them ideal for use in electromagnets, solenoids or relays.

4 Magnetic anisotropy

The magnetic properties of crystals are modified and controlled by magnetic anisotropy. It is the dependence of the internal energy or the free energy density compared to the spontaneous orientation of magnetization with respect to the crystal axes. The energy of the system is minimum or maximum for magnetization lying along a particular direction known as an easy or hard axis of magnetization respectively [14]. Magnetic anisotropy typically results from two types of interaction :

* The spin-orbit coupling and the crystalline field that pair the magnetization to the crystal network, which is the origin of the magneto-crystalline and magneto-elastic anisotropy.
* The dipolar interaction between magnetic moment, whose range is clearly large, which is at the origin of the dipole anisotropy (shape, surface or interface)

The magnetic anisotropy can be intrinsic e.g. magneto-crystalline anisotropy, or

extrinsic e.g. magneto-elastic anisotropy and shape anisotropy.

4.1 Magneto-crystalline anisotropy (MCA)

This anisotropy arises from spin-orbit coupling, where it describes the internal dependence of energy on the direction of the spontaneous magnetization [14]. The electronic orbitals are highly directional as determined by the symmetry of the crystal (due to lattice-orbital coupling) [15]. This tends to align the spin along some specific direction, with respect to the lattice axes, which is determined by the orbital orientation. Spin alignment along this direction corresponds to the minimum energy configuration of the system. Alignment of the magnetic moment along a direction different from the easy axis results in an increase in the energy of the system, which reach its maximum when the direction is along a hard axis. There are two different types of magneto-crystalline anisotropy depending on the crystal structure : uniaxial anisotropy and cubic anisotropy.

4.2 Shape anisotropy

The magnetic dipolar anisotropy, or shape anisotropy, is mediated by the dipolar interaction. By analogy with the electrostatics, the magnetization creates a dipolar field on the macroscopic scale that opposes its orientation. It's like the magnetic system form a domain with super-magnetically masses appearing at its borders and creates a dipolar field opposed to magnetization. The dipolar field is zero in the large direction and becomes important in the small dimension direction [16].

4.3 Stress anisotropy

In addition to magneto-crystalline anisotropy, there is another effect related to spin orbit coupling called magneto-striction. The magneto-striction arises from the stress due to the deformation of the meshes. The magnetic moment being strongly linked to the atomic orbital, any deformation of the network crystalline under the action of an external stress induces a modification of the magnetic properties. This deformation can even alter the material magnetization direction [14].

5 Exchange interaction

The magnetic moments (or spins) are able to interact with the neighbours moments and assume a specific orientation. The driving force for aligning the different spins arises from exchange interaction between the spins which is of a

quantum mechanical origin. There are various types of exchange interaction from direct to indirect interaction. In the direct interaction the neighbouring spins interact directly with each other, the systems with itinerant magnetic moment can be considered as a best example. In many cases the direct exchange is unverified because the distance between the spins, in that cases the spins can interact through some inter-mediatory and the interaction is termed as indirect exchange with three basic type : the super exchange, RKKY exchange and double exchange. Where :

1. Super exchange : Is the interaction between two magnetic ions separated by a non-magnetic ion, which has been observed in antiferromagnetic insulators.
2. Ruderman-Kittel-Kasuya-Yosida (RKKY) interaction : It is the dominant exchange interaction in metals where there is little or no direct overlap between neighbouring magnetic electrons. It therefore acts through an intermediary which in metals are the conduction electrons. This type of exchange was first proposed by Ruderman and Kittel [17] and later extended by Kasuya and Yosida to give the last version of the RKKY interaction theory.
3. Double exchange : This is the interaction between magnetic ions of mixed valence via non-magnetic ions. Examples of this are alloys containing Mn atoms.

Chapter II

Heusler alloys

Introduction

Spin electronics, or as it is known Spintronics is a new field of material science, that take advantage of the spin and the charge of electron to save and carry informations. The development of Spintronics requires the use of high spin polarization materials with low damping coefficients. Half-metals, characterized by a 100% spin polarization at the Fermi level presenting low resistance for one spin channel and high resistance for the other channel, leading to an enormous potential for using in Spintronics components such as magnetic random access memories (MRAM). There are several types of materials, such as Fe_3O_4 [18] and CrO_2 [19], that have been investigated and predicted to be half metals at low temperature. There is a another type of materials, the so-called Heusler alloys, that are extremely promising for Spintronics application, having a very high Curie temperatures [20] and offering the possibility of possessing the half-metallic character at room temperature [9] [21].

The Heusler compound are one of the most exciting material classes that have a long history in magnetism, starting more than 100 years ago with the detection of the ternary metallic compound Cu_2MnAl by Fritz Heusler in 1903 [8]. Remarkable for the fact that, in certain proportions, they are ferromagnetic, although the constituents are not ferromagnetic. However, it took three decades before explaining that their structure is one for an ordered compound. The first Heusler alloys studied were of the form X_2YZ, where X and Y are a transition metal and Z is an atom from III, IV and V group of the periodic table. Figure II.1 shows an overview of possible combination of elements forming these materials. Until now there are more than 1000 different Heusler compound that have been discovered [22]. The half-metallic ferromagnetic nature is the driving force for the intense study of these compound. The half metals are considered as an hybrids between metals and

semiconductors. In other word they are semiconducting for electrons of one spin orientation, whereas they are metallic for electrons with the opposite direction [2]. With this half metallic character the materials are an important candidate for Spintronics application.

This chapter is a short review of structural, electronic and magnetic proprieties of the Heusler alloys precisely the full Heusler compounds with the half-metallic character.

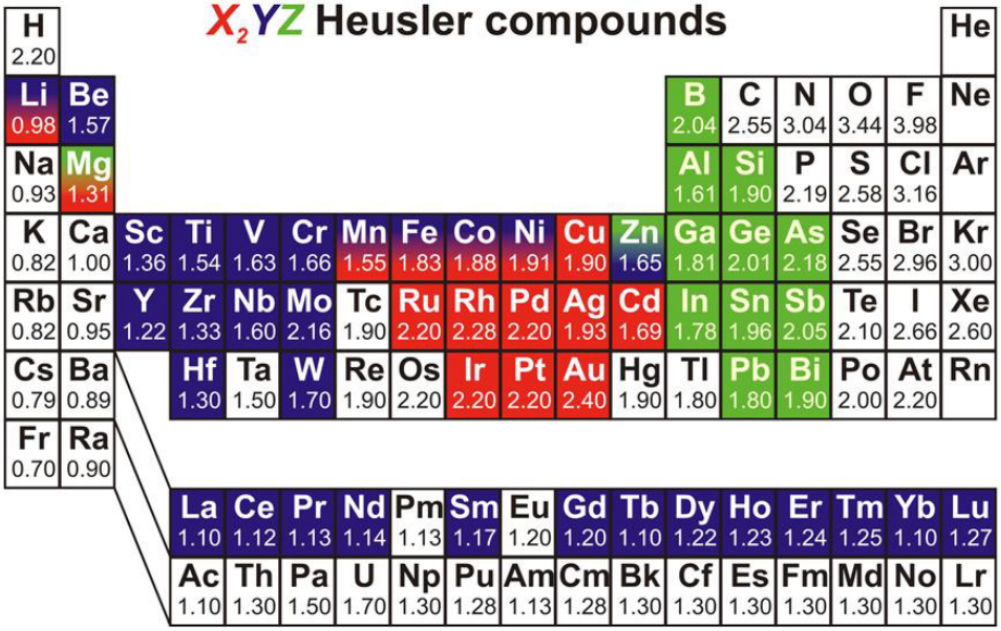


Fig. II.1 – Periodic table of the elements. The huge number of Heusler materials can be formed by combination of the different elements according to the colour scheme.(adopted from [2])

.

1 Crystal structure of Heusler alloys

The Heusler alloys are defined as ternary inter-metallic compounds with the general formula of X_2YZ where X and Y are transition metal atoms and Z is a main group sp-element. The full Heusler alloys are crystallized in the $L2_1$ structure, belonging to the 225 (Fm-3-m) space group, which consists of four inter-penetrating fcc sub-lattices. The X atoms placed on 8c(1/4,1/4,1/4) and the Y and Z atoms on 4a(0,0,0) and 4b(1/2,1/2,1/2) Wyckoff positions respectively. The cubic $L2_1$ structure consists of four inter-penetrating fcc sub-lattice, two equally occupied by X. The two X fcc sublattices combine to form a simple cubic sub-lattice. The Y and Z atoms occupy alternating the centre of simple cubic sub-lattice resulting CsCl type super structure. Which refer to Each Y or Z atom, sitting in an octahedral symmetry position, has eight X atoms as first neighbours, while each X has four Y and four Z atoms as first neighbours and thus the symmetry of the crystal is reduced to the tetrahedral one. The X atoms occupying the two different sub-lattices are chemically equivalent as the environment of the one sub-lattice is the same as the environment of the second one rotated by 90°. Although in the $L2_1$ structure, the X atoms are sitting on second neighbour positions, their interaction is important to explain the magnetic properties of these compounds.(See Figure II.2)

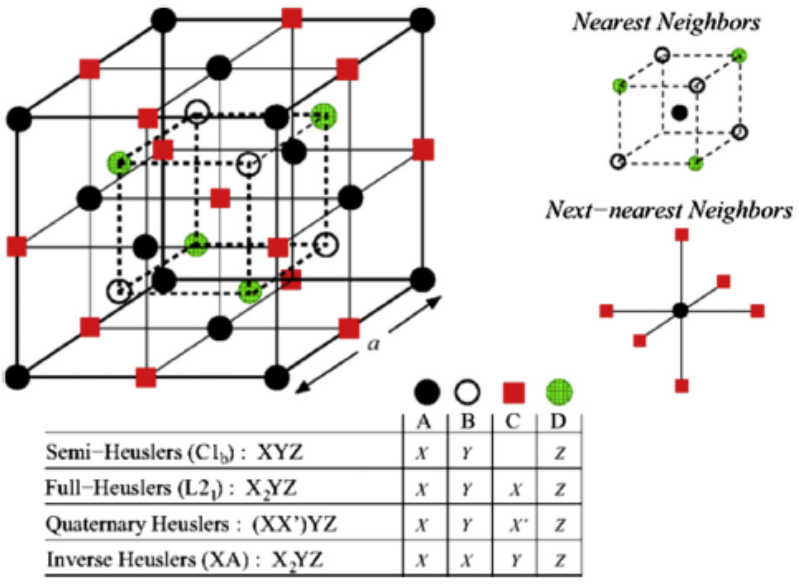


Fig. II.2 – Schematic representations of the various structures of the semi- and full-Heusler compounds. In all cases the lattice is consisted of 4 interpenetrating fcc. lattices. Note also that if all atoms were identical, the lattice would be simply the bcc.(adopted from [3])

.

Moreover there exist so-called half-Heusler phases with the general formula XYZ, having $C1_b$ structure, belonging to 216 space group (F43m) which is a ternary ordered variant of the CaF_2 structure and can be derived from the tetrahedral ZnS type structure by filling the octahedral lattice sites. A characteristic feature of this Half-Heusler structure type are three inter-penetrating fcc sub-lattices, each of them are occupied by the X, Y and Z atoms. The corresponding occupied Wyckoff positions are 4a(0, 0, 0), 4b(1/2, 1/2, 1/2), and 4c(1/4, 1/4, 1/4) (See Figure II.2). In principle, three inequivalent atomic arrangements are possible within this structure type as summarized in table II.1 [2]

	4a	4b	4c
I	X	Y	Z
II	Z	X	Y
III	Y	Z	X

Tab. II.1 – Inequivalent site occupancies within the C1b-type structure. Atoms on Wyckoff positions 4a and 4c form ZnS-type sublattices ; the atoms on 4b occupy the octahedral holes.(adopted from [2])

.

That type know as half-or semi- Heusler compound. The most-well known semi-Heusler compound is $NiMnSb$.

For many Heusler compounds the ordered $L2_1$ structure is the low temperature equilibrium phase. There exist several structural modifications with different degrees of site disorder of the atoms on the X, Y and Z position in the majority of Heusler alloys like the original one (Cu_2MnAl). At high temperatures the crystal structure is bcc with random occupation of the atoms on the lattice sites of a simple bcc lattice with half of the lattice parameter compared to the L21 structure [23].

The full Heusler especially Co-based compounds with Co_2YZ formula attracted the most attention in the Heusler family, because they are a strong ferro-magnets with high curie temperatures (above 600 k [24]) essential for Spintronics application.

2 Half-metallicity of the Heusler alloys

Half-metal refer to the materials that have a strong asymmetry of the spin resolved band structure. In the minority spin band (spin-down) they show semiconductor or even insulating behaviour, while in the majority spin band (spin-up) the conduction electrons exhibit metallic character as shown in figure II.3. This signifies that the conduction electrons are 100% spin polarized at the Fermi level.

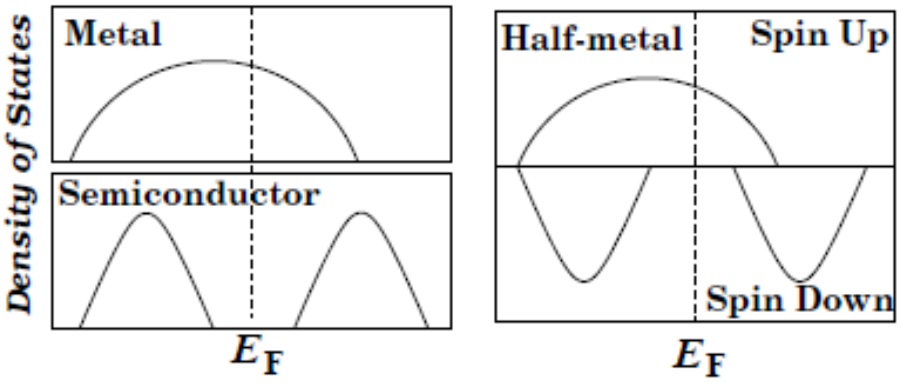


Fig. II.3 – Schematic representation of the density of states for a half-metal with respect to normal metals and semiconductors.

The concept of half-metallic ferromagnetism was first introduced by De Groot et. al based on the band structure calculation for $NiMnSb$ half Heusler alloys [9]. After several theoretical studies they predict the half-metallic character for many other Heusler alloys. The first clear indication of half-metallic ferromagnetism in Co-based Heusler alloys came when Ishida et. al reported the calculated band structure for Co_2MnSi and Co_2MnGe full Heusler alloys(see figure II.4) [4].

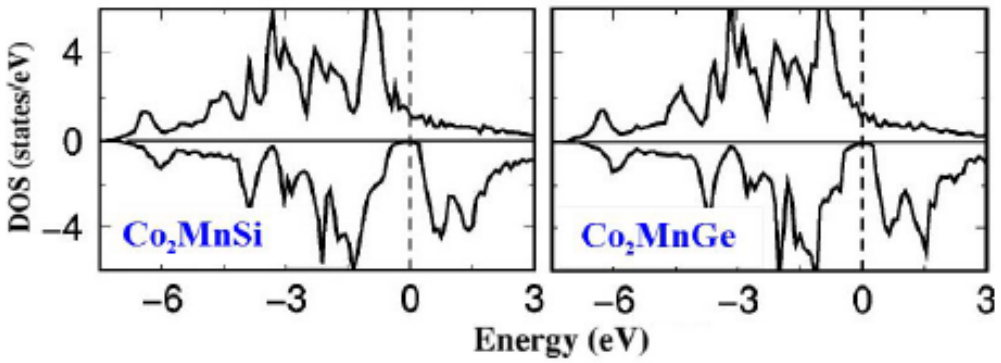


Fig. II.4 – Calculated spin-projected density of states (DOS) for Co_2MnSi and Co_2MnGe. The band gap at the Fermi level for the minority spin band is clearly evidenced.(adopted from [4]).

.

However the half-metallicity has not been founded experimentall, this due to the fact thaty the measured properties are surface and interface sensitive. It has been shown that near surfaces and interfaces the half-metallic property is in most cases lost [25].

3 Origin of half-metallic gap

The prediction of the electronic properties needs to understand the concept of hybridization. The hybridization is a theoretical concept which was introduced by Linus Pauling [26] defining as the mixing of atomic orbitals (ex : s, p, d, f) having the same or slightly different energies to form newly hybridized orbitals (ex :sp, sp^2, sp^3). Hybridization is also an expansion of the valence bond theory (VBT). At almost exactly the same time that chemists were developing the valence-bond model for coordination complexes, an alternative bonding model was applied to transition metal complexes that describe the breaking of orbital degeneracy due to the presence of ligand. This is known as crystal field theory (CFT), where it was originally proposed by Hans Bethe and van Vleck in 1929 [27].

In the crystal field theory, it is assumed that The interaction between the ligands and metal ions (d-orbitals) are considered to be purely electrostatic, and the ligands are considered to be point negative charges. The shape of the five d-orbitals are given in figure II.5.

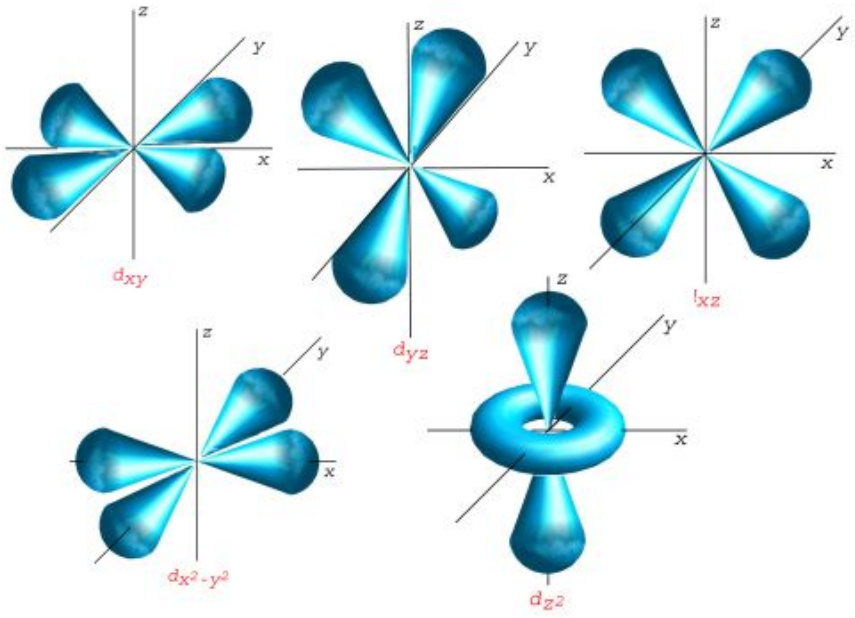


Fig. II.5 – Shapes of d-orbitals.

All the five d-orbitals are degenerate (have the same energy). When they are surrounded by spherically symmetric field of negative charges, the orbitals are raised in energy because of the repulsion between like charges but still being degenerate. In opposite, when ligands approach the metal ion, some experiences more opposition from the d-orbital electrons than others based on the geometric structure of the molecule. Since ligands approach from different directions, not all d-orbitals interact directly, which create a non spherical field that has a lower symmetry. Therefore, the five d-orbitals are no longer degenerate and are split due to the electrostatic environment. This know as the crystal field splitting, where the five d-orbitals are split into two groups : the $d_{x^2-y^2}$ and d_{z^2} orbitals form one set, while the other three orbitals, d_{xy}, d_{yz} and d_{zx} form another set. The former are known as e_g (doubly degenerate) orbitals and the latter are known as t_{2g} (triply degenerate) orbitals (figure II.6).

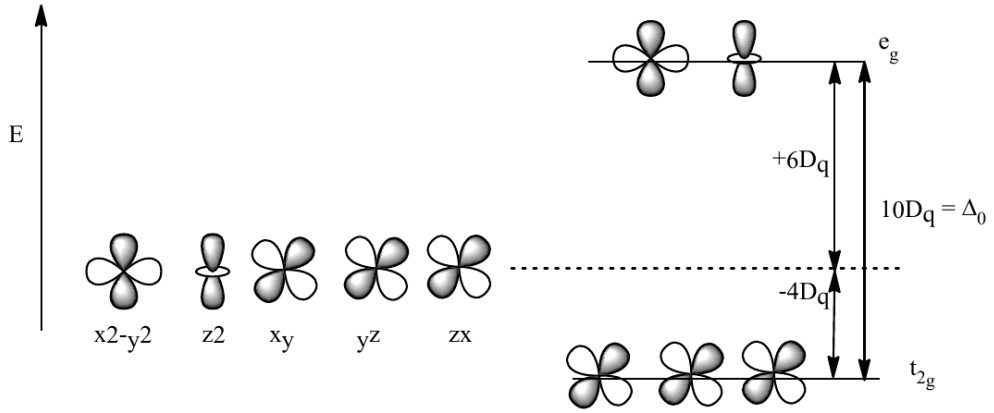


Fig. II.6 – Splitting of d-orbitals. Where 10 Dq or Δ_0 is the energy separation between the two levels, 6 Dq is the amount of repulsion energy needed by e_g orbitals, -4Dq is the stabilization extent needed by t_{2g} orbitals with respect to the barycenter.(Octahedral symmetry)

Basically the gap of full and half Heusler alloys arises from the covalent hybridization between the d-states of the two transition metal (TM) atoms. For the Heusler alloys, the lower-energy d states of the valence band of the TM atom like Ni or Co and the higher energy d states of the conduction band of the TM atom forme the bonding and anti-bonding bands with a gap in between. For the half Heusler as example NiMn the fully occupied 3d orbits of Ni couple with the empty 3d orbital of Mn to form two series of doubly degenerate orbital and triply degenerate orbital, one with a bonding character and the other with an anti-bonding character. Hybridized orbital are separated by a gap. The highest occupied states have essentially a Ni character, while the lower unoccupied states have a strong Mn

contribution. In the other hand, for the full Heusler alloys the origin of the gap was reported by by Galanakis et al. in 2002 [28]. They proposed a model that explain the formation of the minority spin band gap in Co-based full Heusler alloys which result from the Co-Co interaction. In the model the four sp-bands are located far below the Fermi level and thus are not relevant to the gap. So the origin of the gap is attributed to the strong d-hybridization between the two transition metals Co and Mn.(See figure II.7)

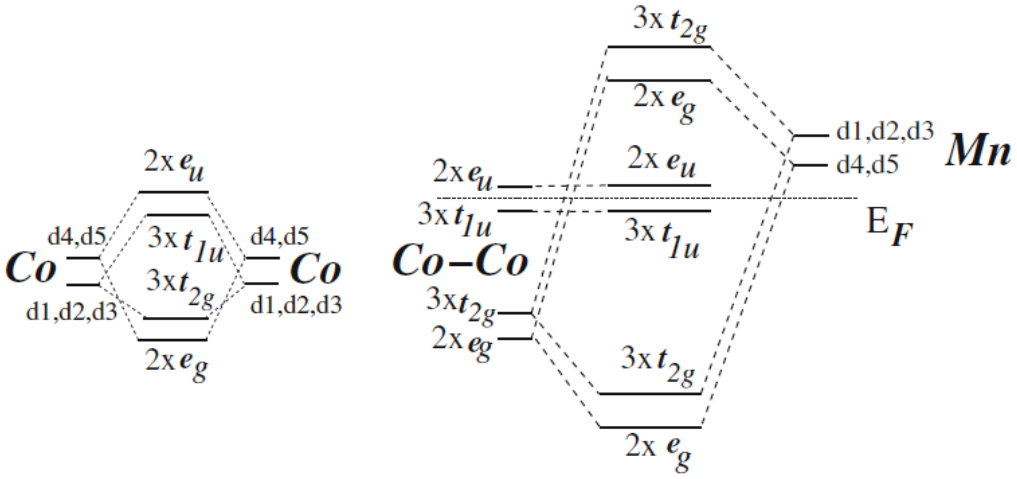


Fig. II.7 – Schematic illustration of the origin of gap in the minority spin band in full-Heusler alloys. For legibility reasons, we use $d1$,$d2$ and $d3$ to denote the d_{xy},d_{yz} and d_{zx} orbitals, respectively, and $d4$,$d5$ for the d_z^2,$d_{x^2-y^2}$ orbitals.(adopted from [24])

The signs $d1$ to $d5$ orbital correspond to the d_{xy},d_{yz},d_{zx},$d_z^2$and $d_{x^2-y^2}$respectively. The $d4$ and $d5$ orbital of the interacting Co atoms form double-degenerated bonding $e_g$and anti-bonding e_u orbital, while orbital form triple-degenerated bonding $t_{2g}$and t_{1u}anti-bonding orbital. It noted that the coupling should be between the orbital with the same character. The double-degenerated e_g orbital hybridize with $d4$ and $d5$ of the Mn transition metal to create a double-degenerated bonding orbital e_g that have a low energy, and an anti-bonding one above the Fermi level. Moreover, the t_{2g} orbital couple with $d1$,$d2$ and $d3$ to form six new orbital, three bonding and three anti-bonding that they have a high energy. The double degenerated e_u and triple-degenerated t_{1u} cannot couple with the d orbital of Mn, since the Mn have no states represent the same symmetries with Co-Co atoms. The Fermi level is found between the e_u and t_{1u} anti-bounding orbital. The gap at Fermi level appears in the minority band. The magnitude of the gap is related to the Co-Co interactions.

4 Magnetic properties

Heusler alloys are systems that possess vast array of magnetic properties, from localized or itinerant magnetism, to anti-ferromagnetism and paramagnetism. The majority of the Heusler alloys with a magnetic element on the Y position order ferromagnetically. The main contribution of the magnetic moment in Heusler compound usually stems from the atoms at the Y position where they are a magnetic element. The moment of the atoms in the X positions is usually small or even dose not exists. There exist a few Heusler compounds with rather large magnetic moments on both the X and the Y positions, the best example for those compounds is the Co_2MnSi and Co_2FeSi. While for the half Heusler the magnetic moment exist only for $X = Mn$ and RE. Because those materials exhibit one magnetic sub-lattice since only the atoms on the octahedral sites can carry a magnetic moment [2]. The mechanism which stabilizes the ferromagnetism is a strong next-nearest neighbour ferromagnetic exchange interaction between the spins at the X and the Y position [28]. If the element that occupies the X position is a non-magnetic element, the dominant exchange interaction between the Y spins is of weaker super exchange type due to hybridization, mediated by the electrons of the non-magnetic Z atoms. Depending on the valence of Z the interaction can have either sign [29].

4.1 Slater-Pauling behaviour

The explanation of the origin of the magnetism of alloys is a complex feature, yet the evolution of the magnetic moment of 3d alloys as a function of valence electrons s per atom can be described in a simple manner using the so-called Slater-Pauling curve [30]. The curve comprises two parts : one for the low valence electron concentrations (localized magnetism), while the other is for the of high valence electron concentrations (itinerant magnetism).(see figure II.8)

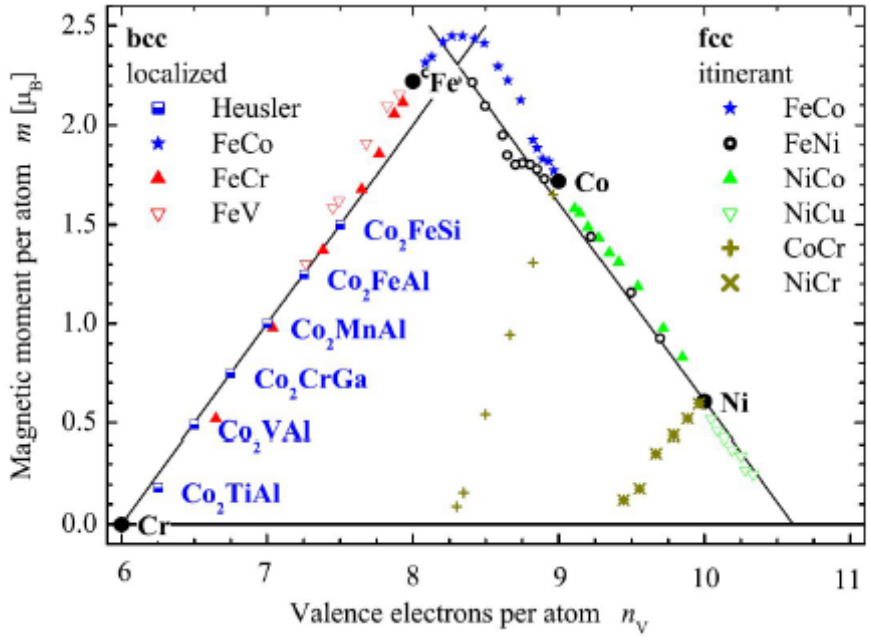


Fig. II.8 – Slater-Pauling curve for 3d transition metals and their alloys. Experimental values for selected Co based Heusler alloys and for binary alloys are also given.

Heusler compounds are situated in the localized part of this curve. Therefore, we focus on this area of the curve. The magnetic moment in multiples of Bohr magnetons given by :

$$M_t = Z_t - 2n_\downarrow$$

Where $2n_\downarrow$ denotes the number of electrons in the minority states.

The number of electrons in the d minority band is approximately three. The magnetic moment in the localized area of the Slater-Pauling curve can be calculated according to :

$$M_t = Z_t - 6$$

Due to the band gap in the minority density of states the number of occupied minority states needs to be an integer, which is exactly fulfilled for the case $M_t = Z_t - 6$. This rule may lead to non-integer values, if the average valence electron concentration is not integer. Thus, it is often more convenient to use the valence electron number per formula unit Z_t [2]

For the Half-Heusler compounds with three atoms per formula unit, the rule is given by :

$$M_t = Z_t - 18$$

While, in the case of full-Heusler compounds there are four atoms per unit cell leading to the formula :

$$M_t = Z_t - 24$$

The half-Heusler alloys (figure II.9) follow the simple rule $M_t = Z_t - 18$. Where the minority population is fixed to 9, so that the screening is achieved by filling the majority band, while in the transition metal alloys the majority band is filled with 5 d-states and charge neutrality is achieved by filling the minority states. The total moment M_t is an integer quantity, assuming the values 0, 1, 2, 3, 4 and 5 if $Z_t \geq 18$. The value 0 corresponds to the semiconducting phase and the value 5 to the maximal moment when all 5 majority d-states are filled. In the case of full Heusler alloys (figure II.9) there are eight occupied minority d states per unit cell : the double degenerated eg with a very low energy, the triple degenerated t_2g orbital and the triple degenerated t_1u that is situated just below the Fermi level .Therefore, there are 12 minority occupied states per unit cell, one with s character, three with p character and eight with d character (2 x e_g, 3 x t_2g and 3 x t_1u), so the total magnetic moment per unit cell must obey the rule $M_t = Z_t - 24$ Since 7 minority bands (2 x Co e_u, 5 x Mn d) are unoccupied, the largest possible moment is 7 μ_B and occurs when all majority d-states are occupied, due to that the co-based Heusler alloys should be placed in the part of the Slater-Pauling curve that corresponds to the localized magnetic moment.

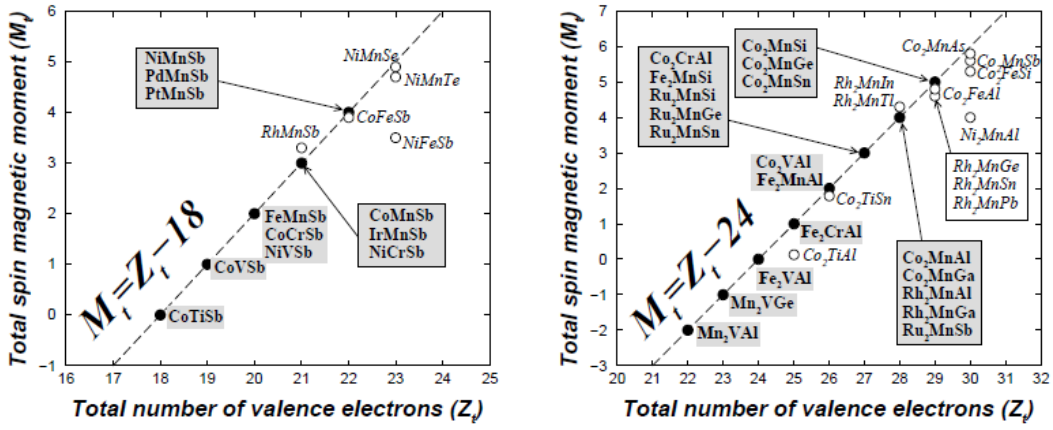


Fig. II.9 – Left panel : Calculated total magnetic moment as a function of the total number Z_t of valence electrons per unit cell for all the studied half Heusler alloys. The dashed line represents the Slater-Pauling behaviour. The open circles present the compounds deviating from the SP curve. Right panel : The same for the full Heusler alloys.

4.2 Exchange interactions

For the full Heusler alloys of X_2MnZ type, the first study considering the exchange interaction and formation of localized magnetic moments was given by kübler et al [29].Due to the large Mn-Mn separation (> 0.4 nm),there is no significant direct interaction between the d states of different Mn. Where in the case of a magnetic X atom the magnetic moment resides on the Mn atom and that the Mn-Mn interaction is mediated by the X sublattice. While for the non-magnetic X atom the coupling of the Mn magnetic moment was thought to be realized through p orbitals of the Z atom that mediate a RKKY type Mn-Mn interaction. because of the large spatial separation of the Mn atoms in Heusler alloys there is an indirect exchange interaction between the d states of different Mn atom. As a result the magnetism in Mn containing systems strongly depends on the number of conduction electrons, their spin polarization, and the position of the unoccupied Mn 3d states with respect to the Fermi level.

Recently [31], for the Co_2MnZ compounds the magnetic moment per Co atom is not negligible around (1 μ_B), while for the Mn atom the magnetic moment situated around (3 μ_B). According to their results, the interaction between Co and Mn gives the leading contribution of the total effective coupling, while for the Co-Co and Mn-Mn interaction is being five times smaller than the other one. That result is different from the one put forward by kübler et al, where the coupling Mn-Mn is dominant

More recent studies [32] confirmed that the strongest interaction is between Co and Y sites, followed by the interaction between Co sites. The exchange interaction between Co and Y sites is connected with the magnitude of the local magnetic moment on the Y site. In the case of large magnetic moment (e.g. Y = Mn) the exchange coupling is the strongest for the Co-Y sublattice, while in the case of small magnetic moment (e.g. Y = Ti) the coupling between Co on different sublattices dominates.

Chapter III

Overview of theoretical framework

1 Density Functional Theory

The ultimate goal for most approaches in solid state physics like ab-initio methods is the resolution of time-independent Schrödinger equation [33]. Those methods make it easy to determine the physical and chemical quantities of a system such as electron structure, density of states..... Since each material contained N particle, the Schrödinger equation become multi-particle equation which make it hard to resolve. Owing to some approximation, the problem simplified in a single-particle equation system. In this chapter will be briefly explained the most usable method for solving these equations.

1.1 Elementary quantum mechanics

1.1.1 Schrödinger equation

The resolution of Schrödinger equation made it possible to study theoretically the different property of materials.

$$\widehat{H}\Psi_i(\overrightarrow{r_i},\overrightarrow{R_j}) = E\Psi_i(\overrightarrow{r_i},\overrightarrow{R_j}) \tag{III.1}$$

$\hat{H}$: Hamiltonian for a system.

r_i : The variables describing the position of the electrons.

R_i : The variables describing the position of the nuclei.

E : The energy of the ground state described by the proper function Ψ.

Usually, the Hamiltonian operator is written as :

$$H_{tot} = T_{nucl}(R) + T_e(r) + V_{nucl}(R) + V_{ee}(R) + V_{e-nucl}(r,R) \tag{III.2}$$

where : T_e and T_{nucl} are the kinetic energy of electron and nuclei, V_{ee} and V_{nucl} the energy of repulsion between electrons and nuclei, V_{e-nucl} is the energy of attraction between nuclei and electrons. This operator can be written by :

$$T_e = -\frac{\hbar^2}{2m}\sum_{i=1}\nabla_i^2 \tag{III.3}$$

$$T_{nucl} = -\frac{\hbar^2}{2M_k}\sum_{k=1}\nabla_k^2 \tag{III.4}$$

$$V_{ee} = \frac{ke^2}{2}\sum_{i,j}\frac{1}{|\vec{r_i}-\vec{r_j}|} \tag{III.5}$$

$$V_{e-nucl} = -ke^2\sum_{i,k}\frac{Z_k}{|\vec{R_k}-\vec{r_i}|} \tag{III.6}$$

$$V_{nucl} = \frac{ke^2}{2}\sum_{K,L}\frac{Z_K Z_L}{|\vec{R_K}-\vec{R_L}|} \tag{III.7}$$

Where : The indices i, j and K, L related to the electrons and nuclei.

k : Coulomb constant.

m : The mass of an electron.

M_k and Z_K : Respectively represent the mass and the charge of the K^{eme} nuclei.

The wave function Ψ depends on the coordinates of all particles, in other world the number of variables for the same type of atom goes to 3N variables, which make the resolution of the equation (III.1) impossible. So ,that lead us to use some approximation.

1.1.2 Born-Oppenheimer approximation

The Born-Oppenheimer approximation [34],take in account that the nuclei move much slower than the electrons due to their masses. For that reason, the movement of the nuclei compared to the electrons may be neglected, which mean nuclei will be considered immovable. In this state, the kinetic energy of the nuclei is zero ($T_{nucl} = 0$) and the potential energy is merely a constant. Thus, the electronic Hamiltonian reduces to :

$$H_{tot} = T_e(r) + V_{ee}(R) + V_{e-nucl}(r, R) \tag{III.8}$$

However, the first problem of 3N variable get to be a problem of N variable, the wave function of the system depends on the coordinates of all electrons and can't be decomposed into contributions of isolated particles because of the latter interact with each other.

The problem is impossible to solve unless it is reduced to a single problem particle. Two possible approximations reduce the problem of N electrons in an effective form to an electron : the Hartree-Fock approximation and the DFT.

1.1.3 The variational principle for the ground state

The variational principle allows us to estimate the energy of the ground state of a system. We chose an un-normalized trial function Ψ which depends on some variational parameters.

$$E = \frac{\langle \Psi | H | \Psi \rangle}{\langle \Psi | \Psi \rangle} \tag{III.9}$$

where $\langle \Psi | H | \Psi \rangle = \int \Psi \hat{H} \Psi d\vec{x}$

The energy computed from a guessed Ψ is an upper bound to the true ground-state energy E_0. Full minimization of the functional $E(\Psi)$ with respect to all allowed N-electrons wave functions will give the true ground state ψ_0 and energy $E(\Psi_0) = E_0$; that is

$E_0 = min_{\psi \to N} \langle \Psi | T + V_{ee} + V_{e-nucl} | \Psi \rangle$

For a system of N electrons and nuclear potential V_{ext}, the variational principle defines a procedure to determine the ground-state wave function ψ_0, the ground-state energy $E_0[N, V_{ext}]$, and other interested properties. In other words, the ground state energy is a functional of the number of electrons N and the nuclear potential V_{ext} :

$E_0 = E[N, V_{ext}]$

1.1.4 The Hartree-Fock approximation

This approximation [35] consists in supposing that the displacement of the electrons is independent of the average field created by the electrons and the nuclei so this reduces the problem of N electron to a single electron problem. The total Hamiltonian is written as :

$$H = \sum_i H_i \tag{III.10}$$

$$H_i = -\frac{\hbar^2}{2m} \vec{\nabla}_i^2 + V_{HF}(\vec{r_i}) + V_{ext}(\vec{r_i}) \tag{III.11}$$

The first and 3rd terms are the kinetic energy and the potential energy due to the electron-nucleus attraction. V_{HF} is the Hartree-Fock potential.

$$V_{ext}(\vec{r_i}) = -ke^2 \sum_k \frac{Z_k}{|\vec{r_i} - \vec{R_k}|} \tag{III.12}$$

$$V_{HF}(\vec{r_i}) = -\frac{1}{2} \sum_j \frac{e^2}{4\pi\epsilon_0 |\vec{r_i} - \vec{r_j}|} \tag{III.13}$$

The Hartree field makes it possible to reduce the multiple equations to a system of equation with a single electron.

$$[-\frac{\hbar^2}{2m} + V_{HF}(\vec{r}) + V_{ext}(\vec{r})]\phi_i(\vec{r}) = \epsilon_i\phi_i(\vec{r}) \tag{III.14}$$

The electrons must obey the Pauli Exclusion Principle (anti-symmetric), which means the exchange of two electrons in the wave function must cause the appearance of a negative sign :

$$\psi(x_1, x_2) = -\psi(x_1, x_2) \tag{III.15}$$

Which was neglected by Hartree. Fock [36] proposed to write the electronic wave function as a Slater determinant that takes into account the Pauli exclusion principle :

$$\Psi(r_1, r_2, \cdots) = \frac{1}{\sqrt{N!}} \begin{vmatrix} \phi_1(r_1) & \phi_2(r_1) & \cdots & \phi_N(r_1) \\ \phi_1(r_2) & \phi_2(r_2) & \cdots & \phi_N(r_2) \\ \phi_1(r_3) & \phi_2(r_3) & \cdots & \phi_N(r_3) \\ . & . & . & . \\ . & . & . & . \\ . & . & . & . \\ \phi_1(r_N) & \phi_2(r_N) & \cdots & \phi_N(r_N) \end{vmatrix} \tag{III.16}$$

$\frac{1}{\sqrt{N!}}$ represents a normalization constant.

That approximation give a good results, especially in molecular physics, so it can only process systems with few electrons such as small molecules. But, its still not useful because it does not take into account the effects of electronic correlations.

1.2 Density functional theory

The basic concept for the density functional is that the energy of an electrical system interacting in a potential is expressed only as a function of its density. Which introduced by the works of Fermi and Thomas in 1927 [37] [38], that based on the uniform electron gas.

Thomas-Fermi's theory considers an electron system interacting in a coulomb field $V_e(r)$ created by the set of fixed nuclei, having a total energy determined by an approximation theory, where they proposed the kinetic energy of an electron gas depends only on the density of the electrons.

$$T_{TF}[\rho(\vec{r})] = \frac{3}{10}(3\phi^2)^{\frac{2}{3}} \int \rho^{\frac{5}{3}} d\vec{r} \tag{III.17}$$

The energy of an atom is finally obtained using the classical expression for the nuclear-nuclear potential and the electron-electron potential.

$$E_{TF}[\rho(\vec{r})] = \frac{3}{10}(3\phi^2)^{\frac{2}{3}} \int \rho^{\frac{5}{3}} d\vec{r} - Z \int \frac{\rho(\vec{r})}{r} d\vec{r} + \frac{1}{2} \int \int \frac{\rho(\vec{r_1})\rho(\vec{r_2})}{r_{12}} d\vec{r_1} d\vec{r_2} \tag{III.18}$$

In order to determine the correct density to be included in the equation, they employed a variational principle. They assumed that the ground state of the system is connected to the for $\rho(\vec{r})$ which the energy is minimized under the constraint of

$$\int \rho(\vec{r})d\vec{r} = N \tag{III.19}$$

However, this model had some weak points. Afterwards, other scientist such as Slater, Hohenberg and Kohn proposed an exact and more elaborate theory. They formally established the electronic density as the amount describing the electronic system, and established the DFT as the method that determines the density of the ground state.

1.2.1 Hohenberg-Kohn theorems

Hohenberg kohn theorems [39] related to all electronic system that surrounded by an external field $V_e(r)$ such as that induced by the nuclei. These theorems are :

1. The first theorem states that for an interacting electron system, the external potential $V_{ext}(r)$ is a unique function of the electronic density of the ground state $\rho_0(r)$. All the properties of the system are determined by the electronic density of the ground state $\rho_0(r)$.
2. The second H-K theorem states that for any multi-electronic system with an N electron number and an external potential V_{ext}, the functional $E(\rho)$ reaches its minimum value when the electronic density $\rho_0(r)$ corresponds to the exact density of the ground state $\rho_0(r)E(\rho_0) = minE(\rho)$.

That theorem shows that it is possible to write the energy of the system as a functional of the electronic density and also, that this energy obeys the variational principle :

$$E[\rho] = F_{HK}[\rho] + \int V_{ext}\rho(r)d^3r \tag{III.20}$$

Those two previous theorems didn't gave us an indication for the applicability and usefulness of the DFT when it's depend on the form of the functional density $E[\rho]$(polarized system). So we have to find a sufficiently approximation to treat $E[\rho]$

1.2.2 Kohn-Sham equation

Kohn and sham [40] propose to determine the exact properties of a multi-particle system by reducing the problem to a system of mono-electronic equation that can be solved the same way as the H-F method. So they suggested to calculate

the exact kinetic energy of a non-interacting reference system which the same density as the real interacting one.

$$\rho_s(\vec{r}) = \sum_{i=1}^{N} |\phi_i(\vec{r})|^2 = \rho(r) \tag{III.21}$$

The functional of the total energy of Hohenberg and Kohn will be described as :

$$E_s[\rho] = T_s[\rho] + V_s \tag{III.22}$$

Where : (V_s) is the potential in which the electrons move :

$V_s = V_{ext} + V_H + (T - T_s)$

(E_s) is the kinetic energy without interaction given by :

$T_s[\rho] = -\frac{1}{2}\sum_i^N [\langle\Phi_i|\nabla^2|\Phi_i\rangle]$

Kohn and sham equation is :

$$[-\frac{\hbar^2}{2m}\nabla_r^2 + V_s(\vec{r})]\phi_i(\vec{r}) = \epsilon_i\phi_i(\vec{r}) \tag{III.23}$$

$$V_s(\vec{r}) = V_H(\vec{r}) + V_{ext}(\vec{r}) + V_xc(\vec{r}) \tag{III.24}$$

where :

$$V_H(\vec{r}) = ke^2 \int \frac{\rho(\vec{r'})}{|(\vec{r}) - (\vec{r'})|}$$
$$V_{ext}(\vec{r}) = -ke^2 \sum_k \frac{Z_K}{(\vec{r}) - (\vec{R_k})}$$
$$V_{xc}(\vec{r}) = \frac{\partial E_{xc}[\rho(\vec{r})]}{\partial\rho(\vec{r})}$$

ϕ_i and ϵ_i are the orbital and the energies in Kohn Sham equation. The resolution of this equation will give us the density of the ground states.

1.3 The exchange-correlation functional

The term of exchange and correlation is the only mystery in the KS approach, the complexity of that last make it hard to resolve the equation, Nevertheless this functional can be subjected to approximations of the local or near local order of the density.

And for the resolution of that equation we have tow broad approximation.

1.3.1 Local density approximation(LDA)

The basis of all approximate exchange-correlation functional is the Local density approximation(LDA) [41]. The centre of this model is the idea of an uniform electron gas. This is a system in which electrons move on a positive background

charge distribution such that the total ensemble is neutral. Where we can write E_{XC} in the following form

$$E_{xc}^{L}DA[\rho] = \int \epsilon_{xc}[\rho(\vec{r})]\rho(\vec{r})d^3r \tag{III.25}$$

Here,$\epsilon_{xc}[\rho]$is the exchange-correlation energy per particle of a uniform electron gas of density$\rho(\vec{r})$.

The quantity can be split into exchange and correlation contributions.

$$\epsilon_{xc}\left[\rho(\vec{r})\right] = \epsilon_x\left[\rho(\vec{r})\right] + \epsilon_c\left[\rho(\vec{r})\right] \tag{III.26}$$

The exchange part, which represents the exchange energy of an electron in a uniform electron gas of a particular density, was derived by Bloch and Dirac in the late 1920's [42].

$$E_{xc} = -\frac{3}{4}\left[\frac{3}{\pi}\rho(\vec{r})\right]^{\frac{3}{4}} \tag{III.27}$$

The correlation part $\varepsilon_c(\rho)$ can not be expressed exactly. The approximation of that term is derived from quantum Monte Carlo calculations of Ceperley and Alder (1980) [43]. Today, there are numerical or analytic expression of $\varepsilon_c(\rho)$,such as that of Perdew et al [44].

1.3.2 Local spin density approximation(LSDA)

The principle of the LDA where generalized in order to gave the new form LSDA "local spin density approximation" . Where they take an account the two different states of the spin "up and down".

$$E_{xc}^{LSDA}[\rho_{(\downarrow)}, \rho_{(\uparrow)}] = \int \epsilon_{xc}(\rho_{(\downarrow)}, \rho_{(\uparrow)})\rho(\vec{r})d^3r \tag{III.28}$$

However, that approximation can describe correctly the systems with a small variant of the electronic density in space. But fail in systems with big number of electron which lead to a dominated electron-electron interaction effects.

1.3.3 The generalized gradient approximation(GGA)

In order to account the non-homogeneity of the true electron density, we need to go beyond the LDA which use only the information about the density at a particular point, so they introduce a supplement to the density. That was the gradient of the charge density $\nabla\rho(\vec{r})$ [45]. Thus, we write the exchange-correlation energy in the following form termed Generalized Gradient Approximation (GGA).

$$E_{xc}^{GGA}[\rho, \nabla\rho] = \int \epsilon_{xc}[\rho(\vec{r}), \nabla\rho(\vec{r})]d^3r \tag{III.29}$$

or

$$E_{xc}\left[\rho_{(\uparrow)},\rho_{\downarrow}\right]=\int f\left[\rho_{(\uparrow)},\rho_{\downarrow},\nabla\rho_{(\uparrow)},\nabla\rho_{(\downarrow)}\right]dr \tag{III.30}$$

We can separate the terms of exchange and correlation, where there are several expressions that have been proposed. In principle, it is possible to combine them, but in fact only a few combinations are used, among which are those of perdew and his collaborators [46] that we will use in our calculations.

1.3.4 Perdew-Burke-Ernzerh approximation(GGA-PBE)

The PBE approximation [47] is the new version of the GGA approximation whose exchange energy can be determined as an integral of the exchange density

$$E_x^{PBE}(\vec{r})=\int dr\rho(\vec{r})\epsilon_x^{PBE}(\rho(\vec{r}),s(\vec{r})) \tag{III.31}$$

$$\epsilon_x^{PBE}(\rho(\vec{r}),s(\vec{r}))=\epsilon_x^{LDA}(\rho(\vec{r})xF_x^{PBE}(s(\vec{r}))) \tag{III.32}$$

$$F_x^{PBE}(s)=-\frac{8}{9}\int_0^{\infty}ydyJ^{PBE}(s,y) \tag{III.33}$$

where : $J^{PBE}(s,y)$ is the exchange part of the functional PBE.

1.4 Resolution of Kohn-Sham equation

The resolution of Kohn Sham equation requires to choice a basis for wave function that can be taken as a linear combination of orbitals known as Kohn Sham orbitals written in the following form :

$$\phi_m(\vec{r})=\sum C_p^m\phi_p(\vec{r}) \tag{III.34}$$

Where ϕ_p and C_p^m are the basic functions and the development coefficients respectively.

The main reason for the resolution of Kohn Sham equation is the determination of C_p^m for occupied orbitals that minimize total energy.

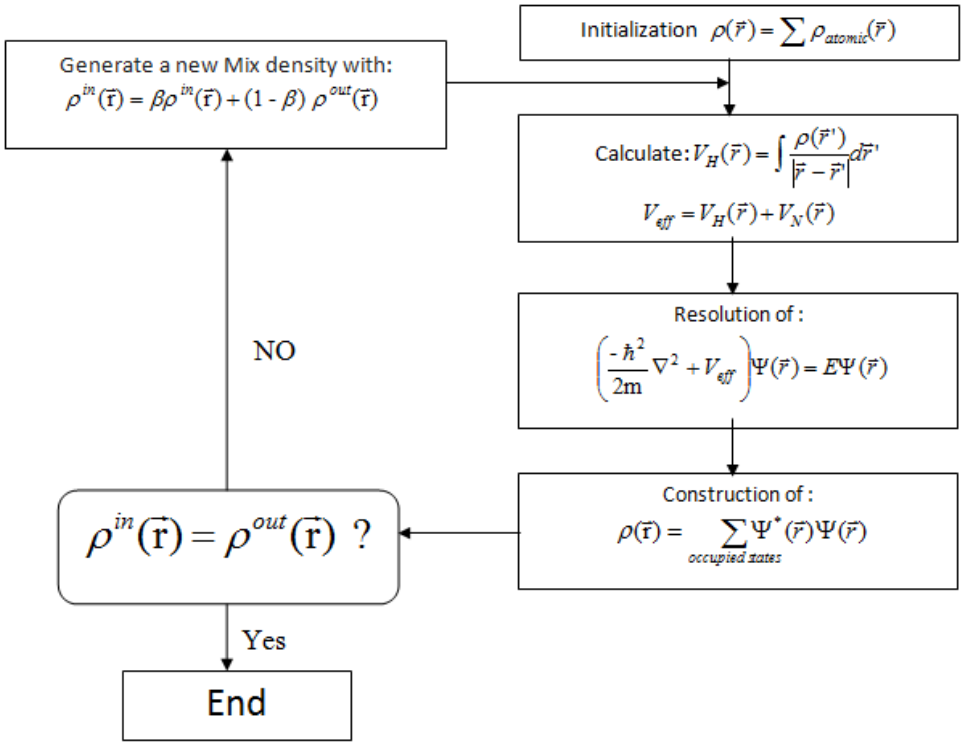


Fig. III.1 – Schematic representation of the self-consistent cycle in the framework of DFT.

The resolution is done in an iterative way using a self-consistent (SC) iteration cycle, We summarize that procedure the following steps (see figure III.1).

1. Start with the injection of a starting density ρ^{in} corresponding to the superposition of the atomic densities of the system.
2. Determination of the V_H and V_{xc}.
3. Solve the Kohn-Sham equation.
4. Construction of the new density.
5. Check the convergence criterion (comparing between ρ^{in} and ρ^{out}).
6. Calculate the different physical quantities (energy, forces, ...) ; end of calculation.
7. If the two quantity of ρ are different, the two densities are mixed and start a new cycle of calculation until we obtained the desired convergence.

2 The Pseudo-potential method (PP)

The Pseudo-potential (or effective potential) method [48] is an advancement of earlier one electron theory of solids [49], where it's considered as one of the simplest tools to study various chemical and physical properties of materials. Such as, the total crystal energy, the respond of solid to the external influences like pressure and the internal energies/vibrations. The term "Pseudo-potential" used by Fermi for the first time [50] to explain the problem of low energy nucleon-nucleon scattering. The basic concepts of Pseudo-potential formalism were developed in 1960's by Phillips and Kleinman [51], as a way to solve Schrödinger equation III.1 for bulk crystals without knowing exactly the potential experienced by an electron in the lattice.

The fundamental concept involved in a Pseudo-potential calculation is that the core electrons are tightly bound to their nuclei where it can be neglected [52], and the valence and conduction band electrons are influenced only by the remaining potential. In other words, a Pseudo-potential is used to reproduce the correct valence charge density outside the core region without treating the core electrons and the atomic nucleus explicitly.

2.1 Bloch's theorem and plane waves

Bloch theorem [53] states that, in a perfect crystal at 0 K, the atoms are positioned regularly and periodically. This periodicity is considering as a characteristic of crystalline potential, so that at any point r we can write :

$$V(\vec{r}) = V(\vec{r} + \vec{R}) \tag{III.35}$$

This expression is the prerequisite for the use of Bloch's theorem. which make it easy to express the wave function of a single particle in a perfect crystal in terms of wave functions of the reciprocal space vectors.

$$\psi_k(\vec{r}) = \exp(i\vec{k}\vec{r}) f_i(\vec{r}) \tag{III.36}$$

Where the vector $\vec{k}$ represents a wave vector in the first Brillouin zone of the reciprocal crystal lattice. The second term of this equation is the periodic wave function within the unit cell.

$$f_i(\vec{r}) = \sum_G C_G(k) \exp(iGr) \tag{III.37}$$

By combining the previews equations we obtain the mono-particle wave function written as a sum of plane waves :

$$\psi_k(\vec{r}) = \sum_G C_G(k) \exp(i(k+G)r) \tag{III.38}$$

To describe a single-particle wave function, we need an infinite number of plane waves. Nevertheless, in practice, this number is limited by a cut-off energy noted $E_{cut-off}$.

2.2 Integration of the Brillouin zone and k points

To calculate the energy of system, it must be integrated in the Brillouin zone (BZ). It is necessary to simplify the (BZ) as finely as possible. Which require a greatly increasing of point and of the time calculation. So to decrease the number of point we use symmetries of system. These points belong to the reciprocal network whose size is inversely proportional to the direct one. So, the bigger it is, the less the reciprocal is, the number of points k necessary for good sampling is therefore lower. In addition, the number of points k in one space direction must also be proportional to that of the others directions.

2.3 General approximation

Because of the strongly relation between the heart electron and the nuclei. So it's considered as immobile electron, which so-called frozen core approximation, by compared to those of valence who is responsible for the most of atom properties. Three large Pseudo-potential families, which are :

Pseudo-potentials called "norm-conserved" standards, the Pseudo-potentials of Vanderbilt called ultra-soft (US-PP) [54], the projected Pseudo-potentials PAW (Projector Augmented Waves) [55].

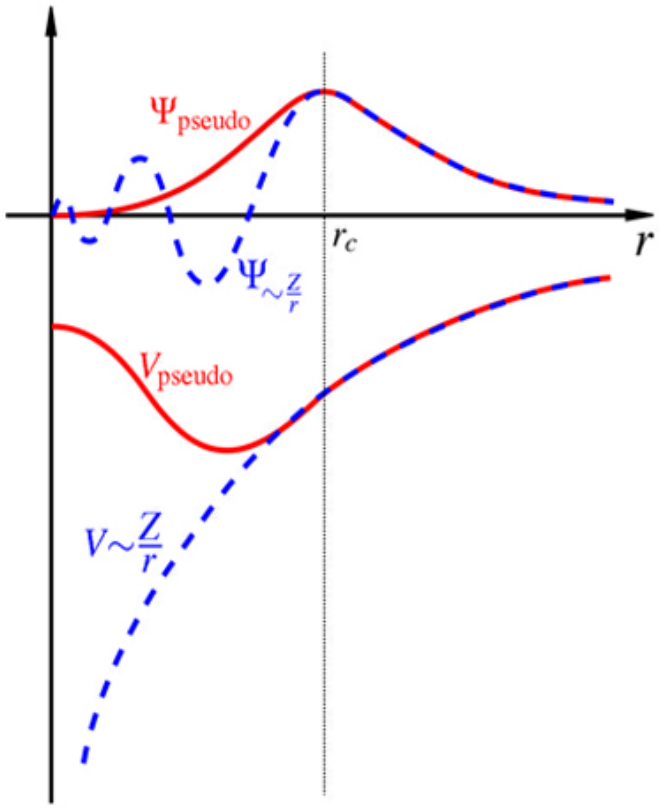


Fig. III.2 – Forms of valence wave functions, pseudo-function, potential of all valence electrons and Pseudo-potential as a function of the atomic radius r.

2.3.1 Norm-conserving Pseudo-potential

The development of these Pseudo-potentials allow for more efficient processing of core electrons and a sharp reduction in cut-off energy. In this method, the charge enclosed in the sphere defined by the cut-off radius must be the same whether it is calculated from the pseudo-wave function or the actual wave function.

2.3.2 Pseudo-potential ultra-soft (US-PP)

This approach was introduced by Vanderbilt [54], the partial wave pseudo-functions are constrained to be equal to the "all electron" wave functions beyond r_c. Below r_c, the pseudo-partial wave function is very soft. As a result, the cut-off radius of the plane wave base can be considerably reduced.

Chapter IV

Results and discussions

Introduction

Recently the full co-based Heusler Co_2MnGe gained a big attention due to their half-metallicity. In this chapter, using the pseudo-potential method, we present the results of calculation of the structural stability, the electronic and magnetic properties of the Co_2MnGe alloys. To define the most stable structure, we calculate the total energy for the different structural phases of Co_2MnGe with all possible positions. Both magnetic and electronic properties were calculated by the GGA for exchange-correlation, which is implemented with the density functional theory (DFT).

The first part of this chapter is dedicated to the determination of the most stable phase structure. In the second part we study the electronic and magnetic properties for this optimized phase. Finally, we discuss the effect of pressure on the structural, electronic and magnetic properties for the Co_2MnGe compound.

1 Computational details

We examined the structure of Co_2MnGe using Density Functional Theory (DFT) as implemented in the CASTEP code. The exchange-correlation is treated with GGA-PBEsol approximation. The geometry optimization is performed under energy per atom convergence criteria equal to 5.0 10^{-6} eV, the maximum force is fixed at 0.01 eV/Å, the maximum stress is limited at 0.02 GPa and the displacement of atoms is fixed at 5.0 10^{-4}Å. The calculation of electronic band structure and density of states were performed with the following criteria : a plane-wave cut-off energy of 350 eV using 8 x 8 x 8 K-mesh in the Brillouin zone which correspond to a 60 irreducible k-points. The set of valance orbitals in the calculations were as 3s, 3p, 4s, 4p, 3d for Co atoms, 3s, 3p, 4s, 4p, 3d for Mn atoms and 3d,

4s, 4p for Ge atoms. All lower states were treated as core states. The result of the structural stability, the magnetic and electronic properties of the Co_2MnGe compound are compared with theoretical studies and existing experimental values. All the calculations were performed using the primitive unit cell.

2 Structural properties

2.1 Crystal structure of Co_2MnGe

The structure of Co_2MnGe adopt the ordered $L2_1$ (space group Fm-3-m), which is the result of four interpenetrating fcc lattices. It is found that the Mn and Ge atoms occupy two fcc sublattices with origin at 4a(0, 0, 0) and 4b(1/2,1/2, 1/2) respectively, the Co atoms are placed on the Wyckoff position 8c(1/4 1/4 1/4) (See figure IV.1). The experimental lattice parameter of Co_2MnGe compound is equal to 5.74 Å [56]. Using this value of the lattice parameter, three different possible configurations for Co_2MnGe(See figure IV.2) are investigated to find the most stable one. The entire possible configuration for Co_2MnGe atoms is noted in the table IV.1.

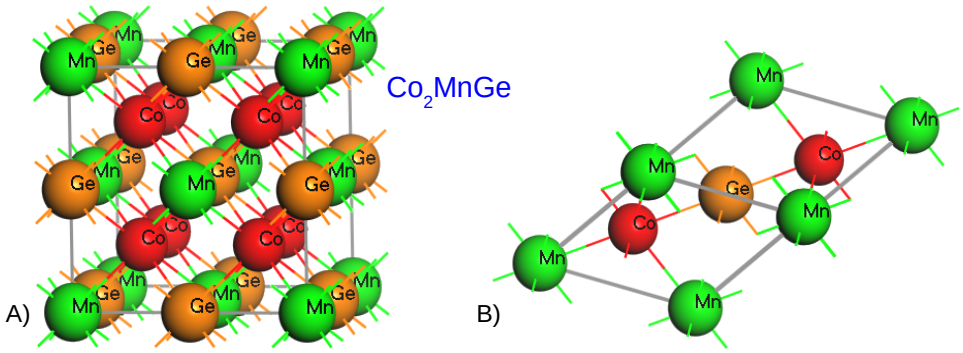


Fig. IV.1 – Structure of Co_2MnGe compound, conventional (left) and primitive cell (right).

	Atoms positions		
Type	Co	Mn	Ge
Configuration I	(1/4,1/4,1/4)	(0,0,0)	(1/2,1/2,1/2)
Configuration II	(1/2,1/2,1/2)	(1/4,1/4,1/4)	(0,0,0)
Configuration III	(0,0,0)	(1/2,1/2,1/2)	(1/4,1/4,1/4)

Tab. IV.1 – Atoms positions in three possible configurations for Co_2MnGe compound.

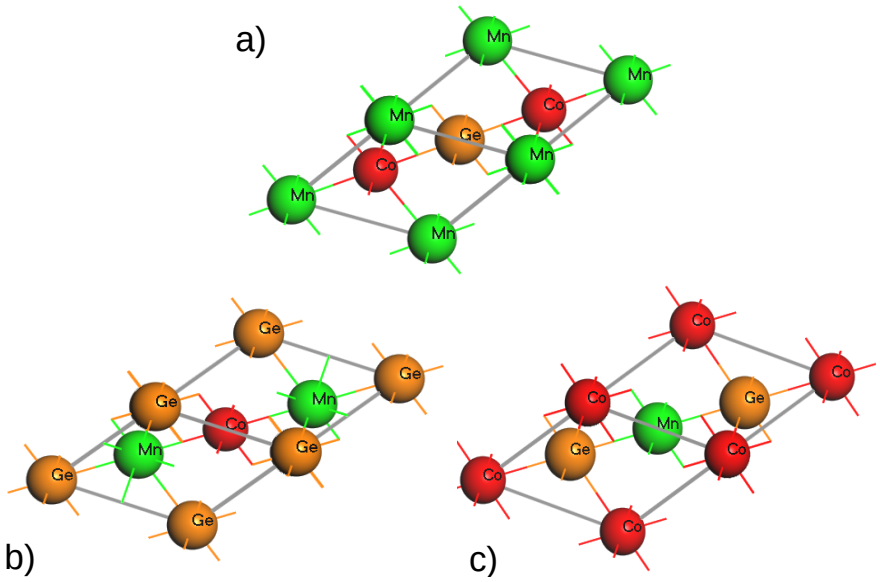


Fig. IV.2 – Crystal structure of Co_2MnGe ternary Heusler compound for (a)-Type I, (b)-Type II, (c)-Type III.

To determine the most stable phase, we have calculated the minimum energy for the three possible configurations of the compound structure, the result are shown in the following table (IV.2).

Configurations	a_{Exp}(Å)	a_{Calc} (Å)	E_{min} (eV)	$Enthalpy * 10^3$ (eV)
I	5.74 [56]	5.7078	-2835.2706	-2.8353
II		5.7810	-2445.7312	-2.4457
III		5.7812	-1903.2593	-1.9033

Table IV.2 – Lattice constants and the equilibrium energy values for the three different configurations.

According to the results cited in the table IV.2, the lowest registered energy among the three structures belongs to the first configuration. The configuration I consequently, corresponds to the most stable phase for our compound. All the characterization for the Co_2MnGe compound, is now mainly based on the first phase structure (Table IV.1).

The energy versus volume curves, for Co_2MnGe compound in it's stable phase, are plotted using Origin software and fitted after defining and compiling a chosen Murnaghan equation of state [57]. The structural parameters like equilibrium energy, lattice parameter and bulk modulus are extracted from a non linear curve fit using the following Murnaghan equation of state (Eq-IV.1).

$$E(V) = E_0 + [\frac{(V_0/V)^{B'}}{B'-1} + 1] - \frac{BV_0}{B'-1} \tag{IV.1}$$

Where :

B is the bulk modulus, it is defined as : $B = V\dfrac{\partial^2 E}{\partial^2 V}$.

$\acute{B}$ is the pressure derivative of the bulk modulus, given by $\acute{B} = \frac{dB}{dP}$.

V_0 is the equilibrium volume in the ground state.

The minimum energy versus volume curves for Co_2MnGe compound are shown in figure IV.3, the red continuous line represents the theoretical fit with the Murnaghan equation of state. The calculated structural parameters are listed in table IV.3.

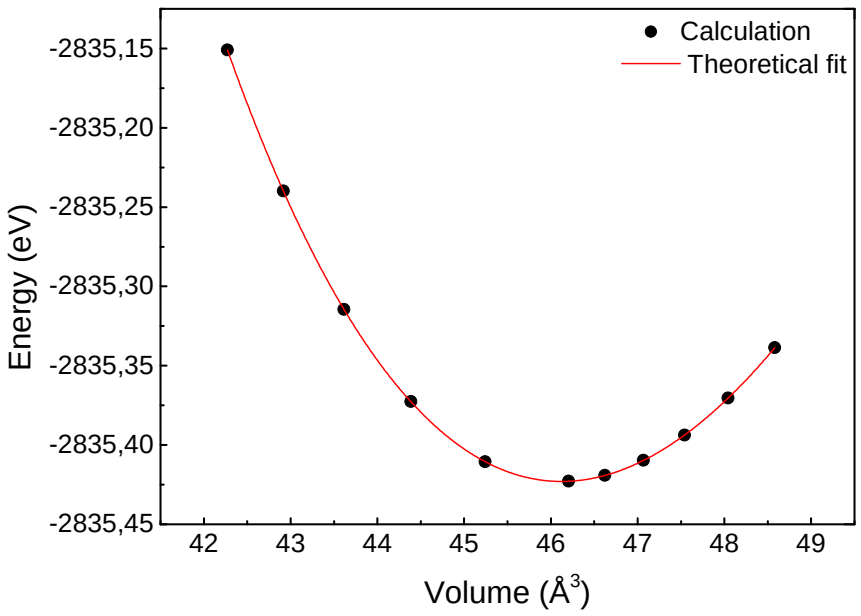


Fig. IV.3 – Total energy as a function of unit volume cell for Co_2MnGe in it's most stable phase I.

a_{Exp} (Å)	a_{Calc} (Å)	$\triangle a$ (Å)	B (GPa)	B'
5.74 [56]	5.6928	0.0472	228.3122	4.8976

Table IV.3 – The calculated bulk parameters of Co_2MnGe in it's most stable phase I.

From the value in table IV.3, we clearly see that the calculated lattice constant agree well with the experimental one. We register a very small difference of about $0.05\mathring{A}$ corresponding to a relative uncertainty of about 0.82%, which is highly acceptable. The bulk modulus express the robustness of the compound.

2.2 Effect of pressure on the volume and lattice parameter

The variation of the lattice parameter and volume for the primitive cell as function of the hydrostatic pressure is plotted in figure IV.4.

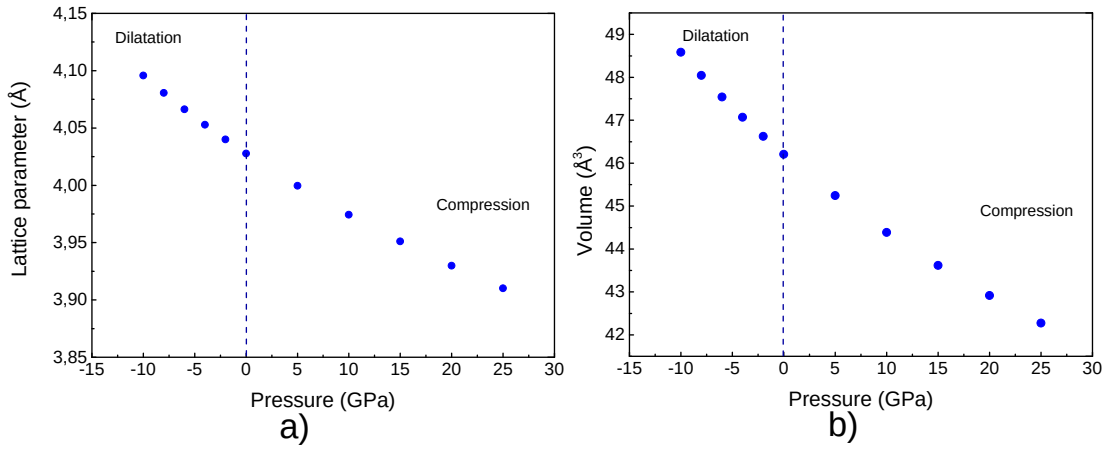


Fig. IV.4 – Lattice parameter (a) and volume (b) of the primitive cell versus pressure.

The plotted curve shows that both values of volume and lattice parameter decrease with increasing pressure from negative values which indicate the dilatation area to the positive values which indicate the compression area.

3 Electronic properties

Band theory, in solid-state physics is a theoretical model describing the states of electrons in solid materials. Electronic states can have values only within certain specific ranges of energy. The dispersion relation $E(k)$ which represents an important function in the case of semiconductors, allow as to calculate quantities such as the energy gap Eg, the effective mass, the electronic transitions and the width of the valence band ... etc. It is possible to specify the nature of material such an insulator, semiconductor, half-metal and metal from the energy band diagrams.

To determine the electronic properties, the band structures along with the high symmetry directions in the Brillouin zone, are calculated for the majority and minority spin populations in the Co_2MnGe alloy.

3.1 Brillouin zone

In the same way to the Bravais lattice which is divided up into Wigner-Seitz cells in the direct space, the Brillouin zone is defined as the primitive cell in reciprocal space. In other words, the first Brillouin zone is a geometrical construction to the WS primitive cell in the k-space. Where it's gives a simple geometric interpretation of the diffraction condition so-called the Bragg condition.

$$K\left(\frac{G_0}{2}\right) = \left|\frac{G_0}{2}\right|^2 \tag{IV.2}$$

Where K and G are wave vector and the reciprocal lattice vector respectively . Thus the procedure to build up the first Brillouin zone is as follows : Select a vector G from the origin to a reciprocal lattice point. Then Construct a plane normal to the vector G at its mid point. This plane forms a part of the zone boundary. The diffracted beam will be in the direction $\vec{k} - \vec{G}$. Thus the Brillouin construction exhibits all the wave vectors k which can be Bragg-reflected by the crystal.

For Co_2MnGe structure, the first Brillouin zone is shown in figure IV.5.

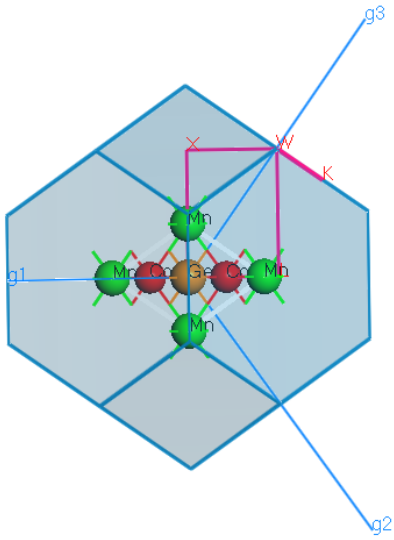


Fig. IV.5 – Brillouin zone of the Co_2MnGe compound ; g_1,g_2 and g_3 are the reciprocal space vectors.

The reciprocal space lattice is characterized by points and directions of high symmetry, along which we have more symmetry to copy a point onto itself. We have points like Γ, K, W, L, X. which correspond respectively to (0,0,0), (3/8,3/8,3/4), (1/2,1/4,3/4), (1/2,1/2,1/2)and (1/2,0,1/2) in the reciprocal space. We have also directions like Δ (100), Λ (111) and Σ (110).

3.2 Band structure

The calculated band structure at along with the high symmetry points and directions in the Brillouin zone for the Co_2MnGe compound are shown in figure IV.6. The energy gap (which is the width of the forbidden band) can be determined from the empty space between the valence the conduction bands.

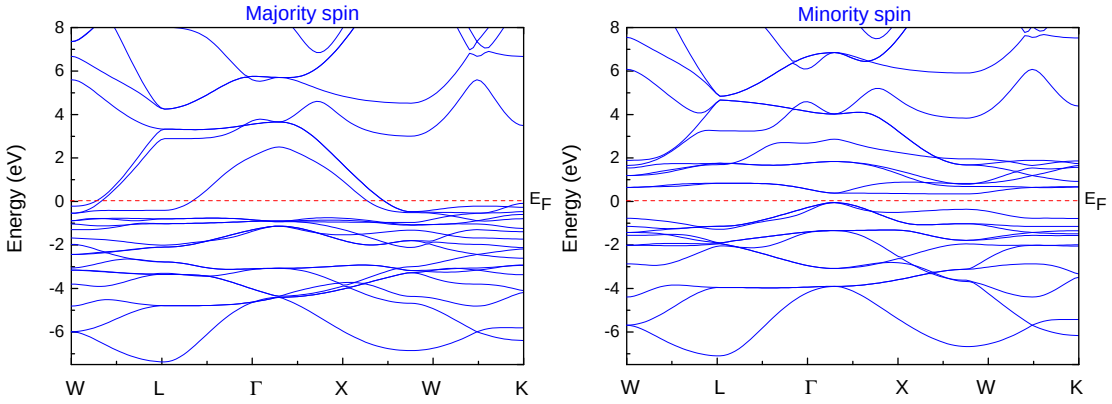


Fig. IV.6 – Band structures curves for Co_2MnGe calculated at zero pressure.

The calculated band structures for Co_2MnGe at 0 (GPa) of pressure is given in the figure IV.6. The two spin populations are depicted too. The spin-up majority population band structure (to left), on one side, shows a Fermi level crossing band, this is an indication of a metallic characteristics. On the other side, the spin down minority band structure exhibit a semiconducting behaviour, an indirect energy band gap of about 0.4027 eV along $\Gamma - W$ points is registered, which is almost similar to another theoretical calculation that indicate an indirect energy band gap along $\Gamma - X$ point about 0.61 eV [58]. The band structure of Co_2MnGe gives evidence for the half-metallicity character of the material.

3.3 Effect of pressure on the energy gap

It should be noted that the hydrostatic pressure significantly affects the value of the energy gaps of materials. The curves in figure IV.7, show the minority spins band structure for Co_2MnGe under different pressure values. We note that :

For the pressure value varying from -2 to -10 GPa, the Fermi level is located at the top of valence band and cross the valence band at -10 GPa, giving rise to a semi-metallic behaviour.

The application of positive pressure values varying from 5 to 25 GPa, the Fermi level drifts away from the valence band to lie in the middle of forbidden band at 15 GPa (figure IV.7-e).

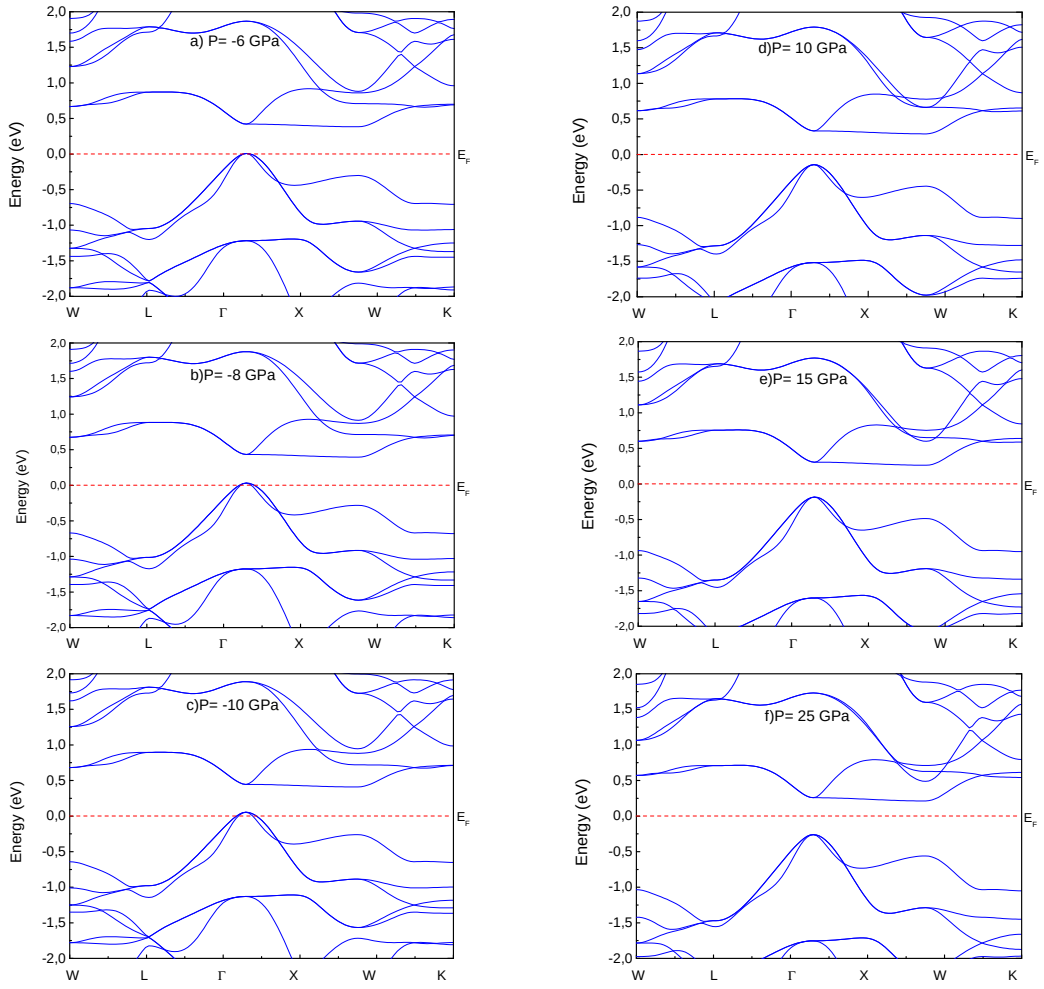


Fig. IV.7 – Band structure of minority spin under different pressure.

The curve in figure IV.8 shows the variation of the energy gap of Co_2MnGe as function of the hydrostatic pressure.

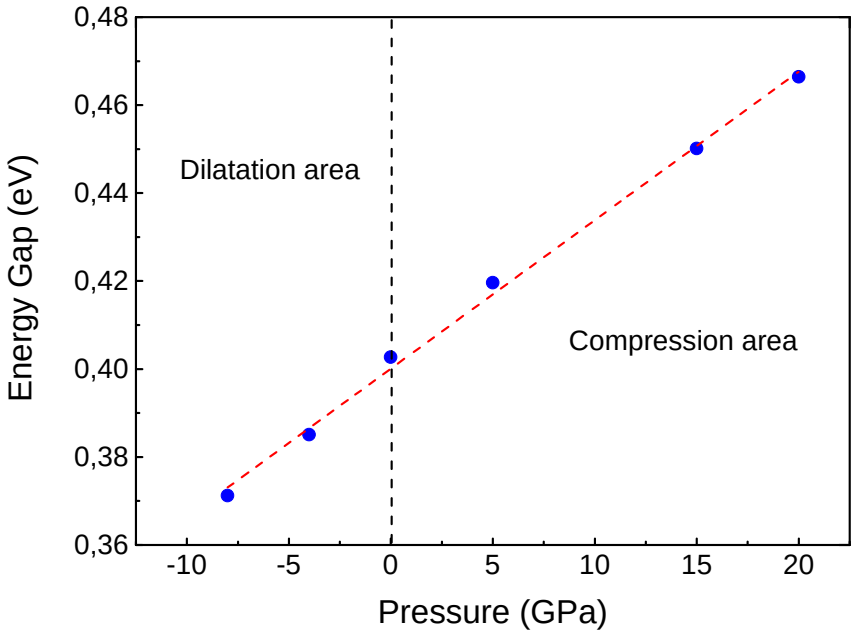


Fig. IV.8 – Variation of the energy gap as a function of pressure.

We see clearly from figure IV.8 that, in the dilatation area which correspond to a negative pressure values, there is a net increase in the gap when the pressure is reduced. Whereas, in the compression area which correspond to a positive values of the pressure, we register a net increase in the gap when the pressure is increased.

The application of strong negative pressure, could destroy the half-metallicity character for the Co_2MnGe, the result is found after extrapolation of the energy gap vs pressure curve which gives a zero value for the gap at about P = -119 GPa leading to the destruction of spin-gap semiconducting character.

3.4 Total and partial densities of states

To obtain more physical details about electronic properties of Co_2MnGe compound under 0 GPa, The total and partial densities of states for Co_2MnGe are presented in figure IV.9. From the figure we note that the total density of states ranges from about -14 eV to 8 eV.

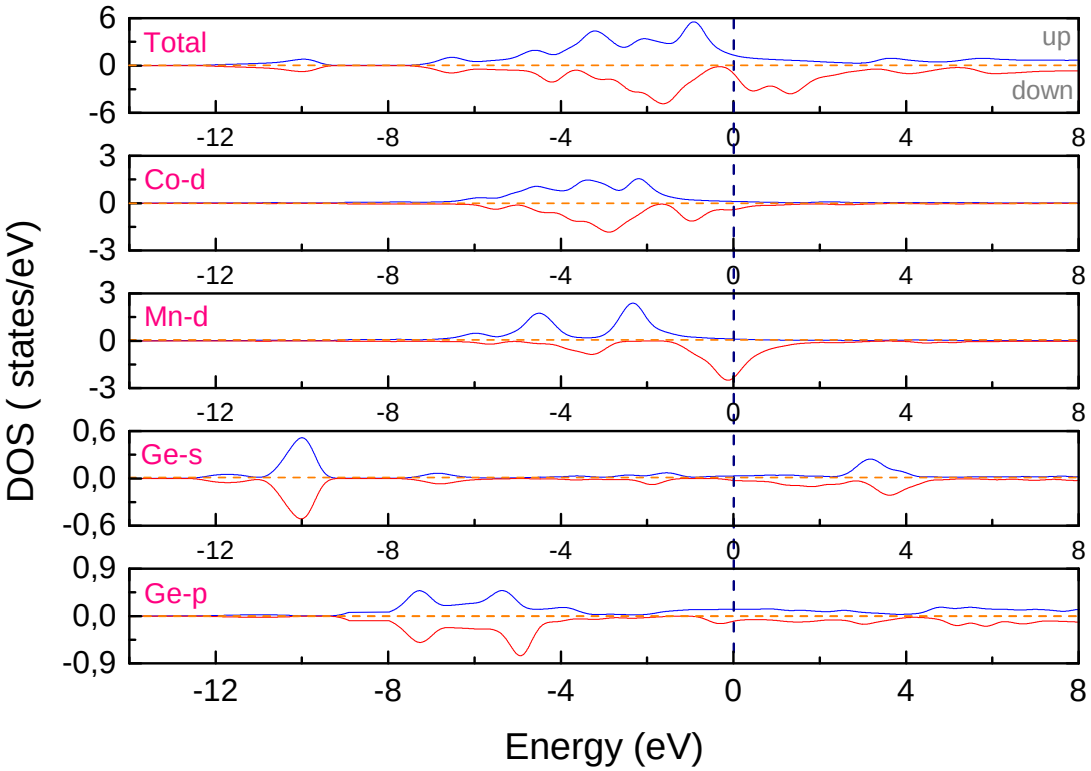


Fig. IV.9 – The total and partial density of states (DOS's) for Co_2MnGe at 0 GPa.

We can be seen that there is a strong hybridization between d-states of Co and Mn. The band gap of Co_2MnGe alloy is determined mainly by this hybridization of the d states between Co and Mn, as well as the Fermi level just located slightly above the conduction band minimum for the minority band spin. Actually, hybridization between d-orbital of transition metals can form minority band gap in Co_2MnGe compound (known as d-d band gap). This type of band gap is the origin of the half metallic character in the full-Heusler alloys. Also we can see from the DOS that the p states of the Ge atom do not directly contribute in the formation of band gap due to the negligible values around the Fermi level, but still contribute in the total density of state for the Co_2MnGe alloy.

4 Magnetic properties

In the case of full Heusler alloys, the total magnetic moment follows the Slater-Pauling rule $M_t = Z_t - 24$ where Z_t represent the number of valence electrons. The Co_2MnGe compound has 29 valence electrons (18 electrons of the two atoms of Co, 7 of the Mn atom and 4 of the Ge atom). Using the Slater-Pauling its total magnetic moment according would be 5 μ_B, the value is in agreement with our calculated total magnetic moment given by the sum of the partial magnetics moments.

The total and partial magnetic moments in the studied Co_2MnGe compound at 0 GPa is shown in table IV.4. As we can see, the most contribution of magnetic moment stem from the Mn atoms. While the two Co atoms have a lower magnetic moment, the Ge atoms have a negligible contribution in the total magnetic moment.

M_t (μ_B)	$m_{Co} * 2$ (μ_B)	m_{Mn} (μ_B)	m_{Ge} (μ_B)
5	0.87	3.34	-0.08

Tab. IV.4 – Calculated values of the total and partial magnetic moment in Co_2MnGe.

4.1 Effect of pressure on the magnetic moment

The change of the magnetic properties for Co_2MnGe as a function of the pressure is indicated in figure IV.10. It should be noted that the total magnetic moment remains constant with compression and expansion of the cell. It can be seen that the change in the pressure does not significantly affect the total magnetic moment in the alloy. However, the partial moment of Co, Mn, and Ge are very sensitive to network distortion. The variation of the magnetic moment of Ge is negligible compared with the magnetic moments of the Co and Mn atoms. The behaviour of Mn magnetic moment with regard to the pressure is opposite to the behaviour of Co and Ge magnetic moments. We see that the partial magnetic moment of Co and Ge increases with the increase of the pressure. At the same time, we notice that the partial magnetic moment of Mn decreases with the increase of the pressure in order to compensate the increase of partial magnetic moments for Co. This can be explained by : The dilatation distortion of the network decreases the hybridization between neighbouring atoms and increases their type of atomic character leading to an increase of their magnetic moments. This behaviour is well known in most Heusler alloys [59].

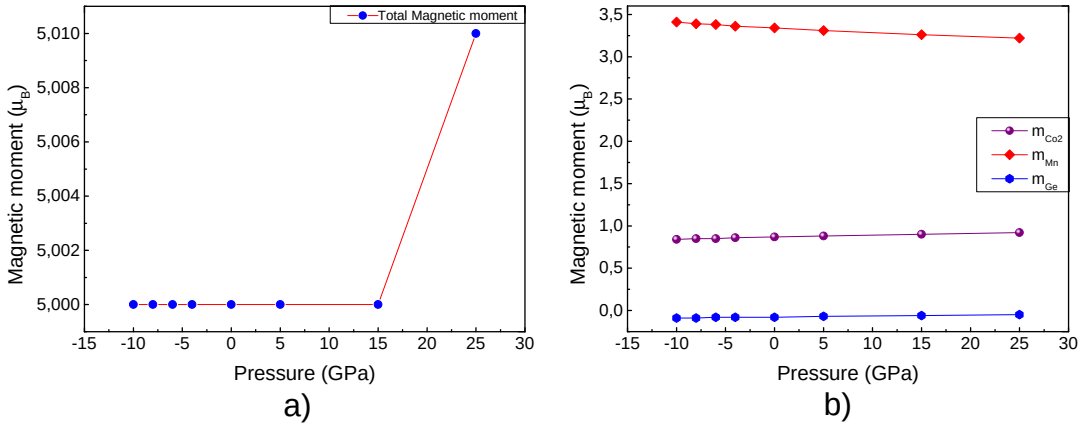


Fig. IV.10 – Total (a) and Partial (b) magnetic moment as function of pressure.

4.2 Spin polarization

One of the features of half-metallic ferromagnets (HMFs) is that, only one spin channel presents a gap at the Fermi level, while the other has a metallic character, leading to 100% carrier spin polarization at Fermi level. To define the quantitative degree of half-metallicity, we introduce the definition of the spin polarization (P). The electron spin polarization (P) at Fermi energy (EF) of a material is defined by [60] :

$$P = \frac{\rho_{\uparrow}(E_f) - \rho_{\downarrow}(E_f)}{\rho_{\uparrow}(E_f) + \rho_{\downarrow}(E_f)} \tag{IV.3}$$

Where $\rho\uparrow$ and $\rho\downarrow$ are the spin density of states, respectively, for the majority and minority spin populations. The table IV.5 lists the obtained polarization at Fermi level and the calculated values of the DOS for spin up and spin down. Results from literature are also cited for comparison.

m_t (μ_B)	$\rho_{\uparrow}$	$\rho_{\downarrow}$	P %
5^c	1.32	0.14	80
5.01 [61]	1.33	0	100

Tab. IV.5 – Calculated total magnetic moment (in μ_B) and spin polarization (P) for Co_2MnGe (5^c represent the present calculation).

It can be seen that, the Co_2MnGe alloy shows a spin polarization of about 80% at Fermi level as can be clearly seen from the density of states in figure IV.11 which confirm the half-metallic nature of the Co_2MnGe compound.

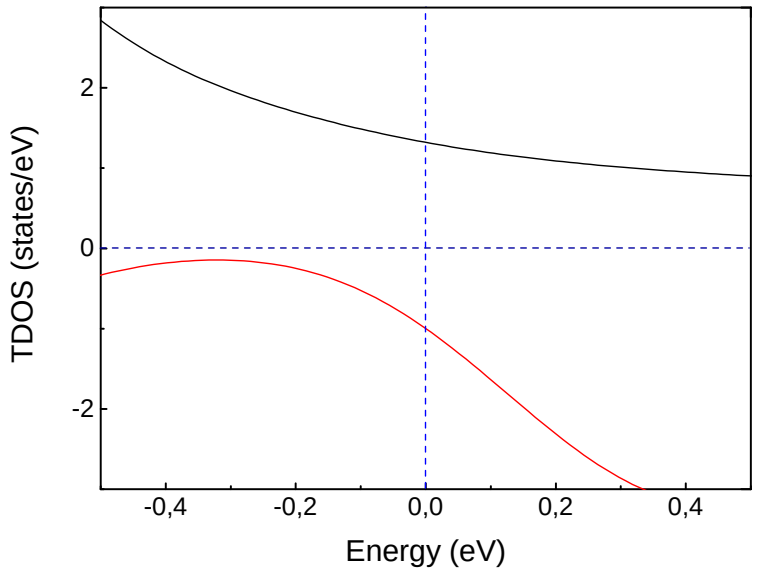


Fig. IV.11 – The amplified curves of the DOS for Co_2MnGe near the Fermi level.

4.3 Effect of pressure on spin polarization

The change in the spin polarization value for the Co_2MnGe as a function of the pressure is indicated in figure IV.12. It should be noticed that the high spin polarization obtained under 0 GPa as shown in table IV.6. On the other hand, we note that the polarization varies with the variation of pressure to create two areas one under the positive pressure, the other for the negative value of pressure.

Pressure (GPa)	-10	-6	-4	0	15	20	25
Polarization(%)	72	77	78	80	76	72	67

Tab. IV.6 – Prominent value of spin polarization as function of pressure.

In the first area for the negative pressure the curves of the density of states (DOS) for the minority and majority spin approach each other as the pressure absolute value decreases, the gap is reduced and high spin polarization is obtained at 0 GPa.

For the positive value of pressure, the gap between the minority and majority spin DOS open up, leading to a minimization in the spin polarization value.

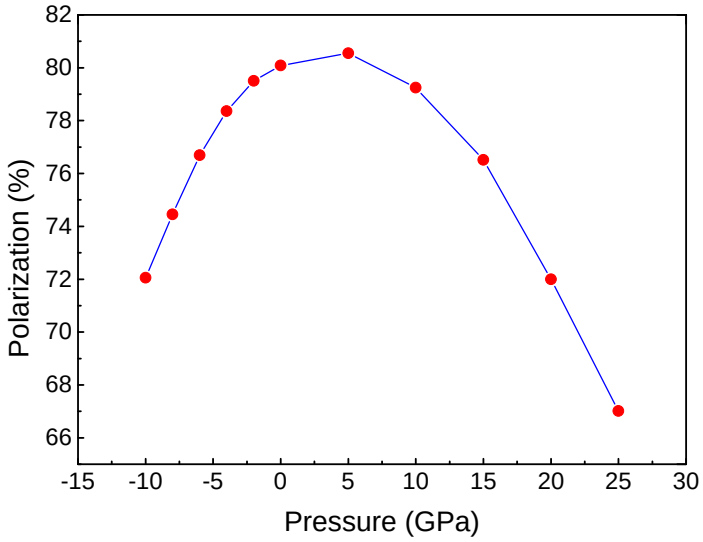


Fig. IV.12 – The curves of spin polarization for Co_2MnGe as function of pressure.

5 Conclusion

In summary, it is confirmed that the half-metallic properties in Co_2MnGe Heusler compound are dominated under 0 GPa pressure. According to the results described here, This material is a semiconductor with narrow indirect gap at 0 GPa for one spin channel, and a conductor for the other spin channel. The calculated magnetic moment $5\mu_B$ is in agreement with the one obtained from Slater-Pauling rule. We also concluded that the spin polarization for that type of material is around 80%.

Conclusion C.

General Conclusion

The study in this dissertation consist of a theoretical investigation of magnetic material. The Co_2MnGe is a full Heusler alloy prototype material. The study is carried out using Density Functional Theory, the exchange-correlation effects are treated using General gradient approximation (PBEsol), Pseudo-potential approximation implemented within CASTEP Code is used for treating an effective potential in the crystal.

For industrial applications of the Spintronics, electrical and magnetic properties play a major role for transport, magnetic detection and magnetic recording technology. It is crucial to understand the influence of pressure, temperature and size on structural, electronic and magnetic properties of materials.Using both electronic and magnetic properties of the electron in the same compound will push one-step farther the developing technologies.

Our aim is the investigation of a new type of material that can make a significant contribution in this field area.

In the first part of the work, we presented an overview on the origin of the magnetic properties and the classification of materials. The Heusler alloys are introduced to bring into light the type and the extent significance of the material we are dealing with.

In the second part of the work, we have focused on one side ; on presenting the theoretical background for the calculation method and all approximations used for the characterisation process. On the other side,the main results are presented and discussed in an attempt to bring light into some corner of shaded area related to the properties of Co_2MnGe full Heusler alloy.

Among three possible structural phases, which correspond to a different positions of atoms in the four fcc sub-lattice of the compound, the most stable phase for our compound is determined using the minimization of energy vs volume curves. We have found that the Co atoms occupy two fcc sub-lattice, a rock salt-type is

formed by the least (Mn) and most (Ge) electropositive element. The structural parameters like lattice constant, compressibility modulus are determined for the most stable phase. The result are in good agreement with experimental values.

The analysis of the density of states clearly show the half metallic character of the Co_2MnGe compound, the results show the existence of a gap at the Fermi level in one spin direction as well as a strongly metallic character in the other direction of spin.

Electronic band structure for our material confirm the half metallic character of the compound, the two spin bands show a completely different behaviour. The majority spin band illustrates the typical metallic behaviour, and the minority spin band exhibits a semiconducting behaviour.

The value of the calculated magnetic moment is in agreement with Slater-Pauling rule for the full-Heusler alloys, at the same time the value of polarization (80%) brings us closer to a the registered half-metallic character of the material.

The application of hydrostatic pressure brings some modification on the structural, electronic and magnetic properties. The lattice parameter and volume decrease with the increasing of pressure. The application of pressure change the value of the energy gap for the minority spin bands, while it does not affect the band structure of the majority spins. Furthermore, we have found that the half metallic character can be destroyed under a specific values of pressure. With the variation of pressure, the total magnetic moment doesn't change, but the partial moment for the constituent elements vary slightly for the Ge atoms and quite strongly for Co and Mn atoms.The value of polarization change slightly with the pressure to preserve the half-metallic nature of the material.

Among the future prospect of this work is understanding how the physical properties of Heusler alloys are correlated with their internal structures (atomic, molecular, crystalline, micro- and macro- scales). Also understanding how these properties are correlated with operational conditions (mechanical, thermal, chemical, electrical and magnetic). More intense if calculations should be held using more powerful equipment to get farther precision and comprehension of the materials which are suitable for application in the rising field of Spintronics.

Bibliography

[1] askIITians, "Magnetic Properties of Materials.." https://www.askiitians.com/iit-jee-magnetism/magnetic-properties-of-materials/. [Online; accessed 23-june-2018].

[2] T. Graf, C. Felser, and S. S. Parkin, "Simple rules for the understanding of heusler compounds," *Progress in solid state chemistry*, vol. 39, no. 1, pp. 1–50, 2011.

[3] I. Galanakis, E. Şaşıoğlu, S. Blügel, and K. Özdoğan, "Voids-driven breakdown of the local-symmetry and slater-pauling rule in half-metallic heusler compounds," *Physical Review B*, vol. 90, no. 6, p. 064408, 2014.

[4] S. Ishida, T. Masaki, S. Fujii, and S. Asano, "Theoretical search for half-metalliic films of co2mnz (zî—» si, ge)," *Physica B : Condensed Matter*, vol. 245, no. 1, pp. 1–8, 1998.

[5] J. Bardeen and W. H. Brattain, "The transistor, a semi-conductor triode," *Physical Review*, vol. 74, no. 2, p. 230, 1948.

[6] M. N. Baibich, J. M. Broto, A. Fert, F. N. Van Dau, F. Petroff, P. Etienne, G. Creuzet, A. Friederich, and J. Chazelas, "Giant magnetoresistance of (001) fe/(001) cr magnetic superlattices," *Physical review letters*, vol. 61, no. 21, p. 2472, 1988.

[7] J. De Boeck, W. Van Roy, J. Das, V. Motsnyi, Z. Liu, L. Lagae, H. Boeve, K. Dessein, and G. Borghs, "Technology and materials issues in semiconductor-based magnetoelectronics," *Semiconductor Science and Technology*, vol. 17, no. 4, p. 342, 2002.

[8] F. Heusler, "F. heusler, verh. dtsch. phys. ges. 5, 219 (1903).," *Verh. Dtsch. Phys. Ges.*, vol. 5, p. 219, 1903.

[9] R. De Groot, F. Mueller, P. Van Engen, and K. Buschow, "New class of materials : half-metallic ferromagnets," *Physical Review Letters*, vol. 50, no. 25, p. 2024, 1983.

[10] A. Akriche, B. Abidri, S. Hiadsi, H. Bouafia, and B. Sahli, "Half-metallic properties and the robustness of co2mnge heusler alloy under pressure : Ab-initio calculation," *Intermetallics*, vol. 68, pp. 42–50, 2016.

[11] R. C. for Magnetic and S. M. (CMSM), "Origin of Magnetism." http://www.nims.go.jp/mmu/tutorials/magnetism.html, 2018. [Online ; accessed 14-mai-2018].

[12] S. Encyclopedia, "Magnetism - Origin Of Magnetism." http://www.nims.go.jp/mmu/tutorials/magnetism.html, 2018. [Online ; accessed 14-mai-2018].

[13] P. Mohn, *Magnetism in the solid state : an introduction*, vol. 134. Springer Science & Business Media, 2006.

[14] H. M. Garad, *L'anisotropie magnétique perpendiculaire induite par oxydation et recuit thermique : de la structure au magnétisme*. PhD thesis, Université de Grenoble, 2012.

[15] J. M. Coey, *Magnetism and magnetic materials*. Cambridge University Press, 2010.

[16] N. GUECHI, *Elaboration et caractérisations structurale, électrique et magnétique des couches minces de F ex N i 100- x déposées sur Si (100)*. PhD thesis, 2015.

[17] M. A. Ruderman and C. Kittel, "Indirect exchange coupling of nuclear magnetic moments by conduction electrons," *Physical Review*, vol. 96, no. 1, p. 99, 1954.

[18] A. Yanase and K. Siratori, "Band structure in the high temperature phase of fe3o4," *Journal of the Physical Society of Japan*, vol. 53, no. 1, pp. 312–317, 1984.

[19] K. Schwarz, "Cro2 predicted as a half-metallic ferromagnet," *Journal of Physics F : Metal Physics*, vol. 16, no. 9, p. L211, 1986.

[20] S. Trudel, O. Gaier, J. Hamrle, and B. Hillebrands, "Magnetic anisotropy, exchange and damping in cobalt-based full-heusler compounds : an experimental review," *Journal of Physics D : Applied Physics*, vol. 43, no. 19, p. 193001, 2010.

[21] H. C. Kandpal, G. H. Fecher, and C. Felser, "Calculated electronic and magnetic properties of the half-metallic, transition metal based heusler compounds," *Journal of Physics D : Applied Physics*, vol. 40, no. 6, p. 1507, 2007.

[22] P. Webster and K. Ziebeck, "Landolt-börnstein new series iii/19c," 1988.

[23] A. Bergmann, J. Grabis, B. Toperverg, V. Leiner, M. Wolff, H. Zabel, and K. Westerholt, "Antiferromagnetic dipolar ordering in [co 2 mn ge/ v] n multilayers," *Physical Review B*, vol. 72, no. 21, p. 214403, 2005.

[24] C. Felser and A. Hirohata, *Heusler Alloys*. Springer, 2015.

[25] I. Galanakis, P. Mavropoulos, and P. Dederichs, "Introduction to half-metallic heusler alloys : electronic structure and magnetic properties," *arXiv preprint cond-mat/0510276*, 2005.

[26] L. Pauling, "The nature of the chemical bond. application of results obtained from the quantum mechanics and from a theory of paramagnetic susceptibility to the structure of molecules," *Journal of the American Chemical Society*, vol. 53, no. 4, pp. 1367–1400, 1931.

[27] J. Van Vleck, "Theory of the variations in paramagnetic anisotropy among different salts of the iron group," *Physical Review*, vol. 41, no. 2, p. 208, 1932.

[28] I. Galanakis, P. Dederichs, and N. Papanikolaou, "Slater-pauling behavior and origin of the half-metallicity of the full-heusler alloys," *Physical Review B*, vol. 66, no. 17, p. 174429, 2002.

[29] J. Kübler, A. William, and C. Sommers, "Formation and coupling of magnetic moments in heusler alloys," *Physical Review B*, vol. 28, no. 4, p. 1745, 1983.

[30] R. C. O'handley, *Modern magnetic materials : principles and applications*. Wiley, 2000.

[31] E. Şaşıoğlu, "E. şaşıoğlu, lm sandratskii, p. bruno, and i. galanakis, phys. rev. b 72, 184415 (2005).," *Phys. Rev. B*, vol. 72, p. 184415, 2005.

[32] J. Thoene, S. Chadov, G. Fecher, C. Felser, and J. Kübler, "Exchange energies, curie temperatures and magnons in heusler compounds," *Journal of Physics D : Applied Physics*, vol. 42, no. 8, p. 084013, 2009.

[33] E. Schrödinger, "An undulatory theory of the mechanics of atoms and molecules," *Physical review*, vol. 28, no. 6, p. 1049, 1926.

[34] M. Born, "Born, m., and r. oppenheimer, 1927, ann. phys.(leipzig) 84, 457," *Ann. Phys.(Leipzig)*, vol. 84, p. 457, 1927.

[35] D. R. Hartree, "The wave mechanics of an atom with a non-coulomb central field. part i. theory and methods," in *Mathematical Proceedings of the Cambridge Philosophical Society*, vol. 24, pp. 89–110, Cambridge University Press, 1928.

[36] V. Fock, "â€žselfconsistent field â€œemit austausch für natrium," *Zeitschrift für Physik*, vol. 62, no. 11-12, pp. 795–805, 1930.

[37] L. H. Thomas, "The calculation of atomic fields," in *Mathematical Proceedings of the Cambridge Philosophical Society*, vol. 23, pp. 542–548, Cambridge University Press, 1927.

[38] E. Fermi, "Eine statistische methode zur bestimmung einiger eigenschaften des atoms und ihre anwendung auf die theorie des periodischen systems der elemente," *Zeitschrift für Physik*, vol. 48, no. 1-2, pp. 73–79, 1928.

[39] P. Hohenberg and W. Kohn, "Inhomogeneous electron gas," *Physical review*, vol. 136, no. 3B, p. B864, 1964.

[40] L. Hedin and S. Lundqvist, "Effects of electron-electron and electron-phonon interactions on the one-electron states of solids," in *Solid state physics*, vol. 23, pp. 1–181, Elsevier, 1970.

[41] R. M. Dreizler and J. da Providência, *Density functional methods in physics*, vol. 123. Springer Science & Business Media, 2013.

[42] P. A. Dirac, "Note on exchange phenomena in the thomas atom," in *Mathematical Proceedings of the Cambridge Philosophical Society*, vol. 26, pp. 376–385, Cambridge University Press, 1930.

[43] D. M. Ceperley and B. Alder, "Ground state of the electron gas by a stochastic method," *Physical Review Letters*, vol. 45, no. 7, p. 566, 1980.

[44] J. P. Perdew and Y. Wang, "Pair-distribution function and its coupling-constant average for the spin-polarized electron gas," *Physical Review B*, vol. 46, no. 20, p. 12947, 1992.

[45] J. Tao, J. P. Perdew, V. N. Staroverov, and G. E. Scuseria, "Climbing the density functional ladder : Nonempirical meta–generalized gradient approximation designed for molecules and solids," *Physical Review Letters*, vol. 91, no. 14, p. 146401, 2003.

[46] J. P. Perdew, J. A. Chevary, S. H. Vosko, K. A. Jackson, M. R. Pederson, D. J. Singh, and C. Fiolhais, "Atoms, molecules, solids, and surfaces : Applications of the generalized gradient approximation for exchange and correlation," *Physical Review B*, vol. 46, no. 11, p. 6671, 1992.

[47] J. P. Perdew, "Jp perdew, k. burke, and m. ernzerhof, phys. rev. lett. 77, 3865 (1996).," *Phys. Rev. Lett.*, vol. 77, p. 3865, 1996.

[48] W. A. Harrison, "Pseudopotentials in the theory of metals," *1966, 336 P. W. A. BENJAMIN, INC., NEW YORK*, 1966.

[49] L. I. IAstrebov and A. A. Katsnelson, *Foundations of one-electron theory of solids*. Amer Inst of Physics, 1987.

[50] E. Fermi *et al.*, "Motion of neutrons in hydrogenous substances," *Ricerca sci*, vol. 7, pp. 13–52, 1936.

[51] J. C. Phillips and L. Kleinman, "New method for calculating wave functions in crystals and molecules," *Physical Review*, vol. 116, no. 2, p. 287, 1959.

[52] U. Von Barth and C. Gelatt, "Validity of the frozen-core approximation and pseudopotential theory for cohesive energy calculations," *Physical Review B*, vol. 21, no. 6, p. 2222, 1980.

[53] N. Ashcroft and N. Mermin, "Solid state physics (saunders college, philadelphia)," *Google Scholar*, p. 404, 1976.

[54] D. Vanderbilt, "Soft self-consistent pseudopotentials in a generalized eigenvalue formalism," *Physical Review B*, vol. 41, no. 11, p. 7892, 1990.

[55] P. E. Blöchl, "Projector augmented-wave method," *Physical review B*, vol. 50, no. 24, p. 17953, 1994.

[56] P. Webster, "Magnetic and chemical order in heusler alloys containing cobalt and manganese," *Journal of Physics and Chemistry of Solids*, vol. 32, no. 6, pp. 1221–1231, 1971.

[57] F. Murnaghan, "The compressibility of media under extreme pressures," *Proceedings of the National Academy of Sciences*, vol. 30, no. 9, pp. 244–247, 1944.

[58] H. Joshi, D. Rai, R. Thapa, *et al.*, "Electronic structure and thermoelectric property of co2yge (y= mn, fe) heusler compounds : a first principle study," in *Journal of Physics : Conference Series*, vol. 765, p. 012010, IOP Publishing, 2016.

[59] I. Galanakis, P. Mavropoulos, and P. H. Dederichs, "Electronic structure and slater–pauling behaviour in half-metallic heusler alloys calculated from first principles," *Journal of Physics D : Applied Physics*, vol. 39, no. 5, p. 765, 2006.

[60] E. Şaşıoğlu, L. Sandratskii, P. Bruno, and I. Galanakis, "Exchange interactions and temperature dependence of magnetization in half-metallic heusler alloys," *Physical review B*, vol. 72, no. 18, p. 184415, 2005.

[61] S. Ouardi, G. H. Fecher, B. Balke, A. Beleanu, X. Kozina, G. Stryganyuk, C. Felser, W. Klöß, H. Schrader, F. Bernardi, *et al.*, "Electronic and crystallographic structure, hard x-ray photoemission, and mechanical and transport properties of the half-metallic heusler compound co 2 mnge," *Physical Review B*, vol. 84, no. 15, p. 155122, 2011.

[62] M. C. Payne, M. P. Teter, D. C. Allan, T. Arias, and a. J. Joannopoulos, "Iterative minimization techniques for ab initio total-energy calculations : molecular dynamics and conjugate gradients," *Reviews of modern physics*, vol. 64, no. 4, p. 1045, 1992.

Abstract :
Spintronics is a new research area dealing with the study of materials harnessing both electron's degrees of freedom (the charge and the spin). The Heusler materials are proposed for achieving such characteristics. The research of a new Heusler compounds leads to the development of half-metallic Ferro-magnets, which are designed as a potential candidate having implications in the efficiency of electronic transport and data storage. A properties of high spin polarization (up to 100%) of the conduction electrons and high Curie temperature were found in *Co*-based Heusler compounds. The aim of this work is to study the structural, electronic and magnetic properties of one full Heusler alloy under the effect of the hydrostatic pressure ($-10 \rightarrow 25GPa$). Using CASTEP code and based on the density functional theory where the exchange and correlation are treated using the GGA approximation, we have carried out a theoretical investigation of the properties of Co_2MnGe compound. The optimized structural results are in good agreement with the experimental studies. The study of the band structures shows the half-metallicity character of Co_2MnGe compound, a high spin polarization of the material is shown from the DOS analyses. For the magnetic properties, the material follows a Slater-Pauling behaviour and its total spin magnetic moment per unit cell is found to be integer and mainly built from the Mn atoms.
Keywords : Spintronics, Heusler alloys, Half-metallicity, GGA , DFT.

Résumé :
La spintronique est un nouveau domaine de recherche qui étudie des matériaux exploitant les deux degrés de liberté de l'électron (la charge et le spin). Les matériaux Heusler sont proposés pour réaliser ce type de caractéristiques. La recherche de nouveaux composés Heusler conduit au développement des semi-métaux ferromagnétiques, qui sont conçus comme des candidats potentiels ayant des implications dans l'efficacité du transport électronique et du stockage de données. Les composés Heusler à base de cobalt ont des propriétés remarquables telles que : polarisation en spin élevée (100%) et une température de Curie importante.

Le but de ce travail est d'étudier les propriétés structurales, électroniques et magnétiques d'un alliage Heusler sous l'effet de la pression hydrostatique ($-10 \rightarrow 25GPa$). En utilisant le code CASTEP, qui basé sur la théorie fonctionnelle de densité où les effets d'échange et de corrélation sont traités par l'approximation GGA, nous avons effectué une étude théorique des propriétés du composé Co_2MnGe. Les proprietés structurales sont en bon accord avec les résultats d'études expérimentales. L'étude de structures de bandes montre le caractére demi-métallique du composé Co_2MnGe, une forte polarisation en spin du matériau est montrée à partir des analyses de la DOS. Pour les propriétés magnétiques, le matériau suit un comportement de Slater-Pauling et son moment magnétique de spin total par cellule primitive est entier et principalement obtenu à partir des atomes de Mn.
Mots-clés : Spintroniques, Alliages Heusler, Semi-métallicité, GGA, DFT, Co_2MnGe.

مُلَخَّص :
سپِنترُونِك هو مَجَالُ بَحث جَديد يَتَمَثلُ في دِرَاسَه المَوَادِ التي تَستَغل كِلَا دَرَجَات الحُرِيَه لِالِكترُون (الشُحنَه وَ اللَّف). تُعتَبَر خَلَائِط هُسلر مِثَاليه لِتَحقيق هَاتِهِ الخصَائِص. اَلبَحت عن خَلِط هُسلر جَديدَ يُؤَدِي إِلَي تَطوير انصَاف المَعَادِن الفيرُمغنَاطِسِيَه، وَ الَّتِي تُعَدُ كَمُرَشَح كُفُؤ لِنَقل وَ تَخزين البَيَانَات. في مُرَكَبَات هُسلر الَتي تَشتَمِل عَلَ كُوبَالت تَمَ العُثُر عَلَ استِقطَابِيَه عَالِيَه تَصِل إِلَ ١٠٠ % تَحتَ دَرَجَه كُوري مُرتَفِعَه.

اَلهَدَف مِن هذَا العَمَل هو دِرَاسَه الخَصَائِص البُنيَوِيَه، اَلاِلِكترُونِيَه وَ المِغنَاطِسيَه لِخَلَائِط هُسلر تَحتَ تَاثِير الضَغط الهِيدرُوستَاتِيكِي ($-10GPa \leftarrow 25$). بِاستِخدَام بَرنَامَج كَاستِب وَ بِنَاءَ عَلي نَظَرِيَه دَالِيَه الكَثَافَه حَيث يتمُ التَعَامُل مَع التَبَادُل وَ الاِرتِبَاط بِاستِخدَام (جي جي يَاَ) ، حَيث قُمنَا بِاجرَاء دِرَاسَه نَظَرِيَه لِخَصَائِص Co_2MnGe . تَتَوَافَق نَتَائِج الخَصَائِص البُنيَوِيَه المُتَحَصَل عَلَيهَا مَعَ الدِرَاسَات التَجرِيبِيَه. وَ تُظهِر دِرَاسَه نِطَاق البُنيَه خَاصِيَه نِصف المَعَادِن لِمُركَب Co_2MnGe ،كَمَ وَ تَظهَر إِستِقطَابِيَه المُرَكَب مِن خِلَال تَحلِيل مُنحَنَيَات كَثَافَته الحَالَه. بِالنِسبَه لِلخَصَائِص المِغنَاطِسيَه ، تَتَبع المَادَه سُلُوك سلَاتِر بَاولِن، وَ تَبَيَن أَن العزم المِغنَاطِسي الكُلِي في الخَلِيَه الوَاحِدَه يَتَمَركَز في ذَرَات مَنغَنِيز.
اَلكَلِمَات المِفتَاحِيَه : سپِنترُونِك، خَلَائِط هُسلر، نِصف المَعَادِن، نَظَرِيَه دَالِيَه الكَثَافَه.



UNIVERSITY YAHIA FARES